Development sustainable concrete with high-volume wastes tile ceramic: Role of silica nanoparticles amalgamation

Zahraa Hussein Joudah [a,b], Nur Hafizah A. Khalid [a,*], Mohammad Hajmohammadian Baghban [c,*], Iman Faridmehr [d], Adrina Rosseira A. Talip [a], Ghasan Fahim Huseien [e,f,**]

[a] Faculty of Civil Engineering, Universiti Teknologi Malaysia, Johor Bahru, Johor 81310, Malaysia
[b] Department of Civil Engineering, Faculty of Engineering, University of Misan, Amarah 62001, Iraq
[c] Department of Manufacturing and Civil Engineering, Norwegian University of Science and Technology (NTNU), Gjøvik 2815, Norway
[d] Civil Engineering Department, Faculty of Engineering, Girne American University, N. Cyprus Via Mersin 10, Turkey
[e] Guangzhou Institute of Energy Conversion, Chinese Academy of Sciences, Guangzhou, Guangdong 510640, China
[f] Department of the Built Environment, School of Design and Environment, National University of Singapore, 117566, Singapore

ARTICLE INFO

ABSTRACT

As the global concrete industry shifts towards sustainable practices, there is an increasing focus on mitigating the environmental impacts of ordinary Portland cement (OPC)-based concrete, which is notorious for its significant greenhouse gas emissions, high energy consumption, and substantial demand for natural resources. This urgency is compounded by the growing production of waste tile ceramic materials due to rapid urban development, leading to enhanced research into their recyclability within concrete for improved durability and sustainability. This study explores the development of high-strength concrete utilizing waste tile ceramic aggregates (WTCAs) and waste tile ceramic powder (WTCP) as replacements for natural aggregate and OPC, respectively. To further enhance the concrete's mechanical properties and microstructure, silica nanoparticles derived from waste bottle glass (WBGNPs) were integrated in varying proportions ranging from 2 % to 10 % of the binder content. Optimal results were achieved with a full replacement of natural aggregate by WTCAs, 60 % substitution of OPC by WTCP, and the inclusion of 4 % WBGNPs, which collectively exhibited superior compressive, splitting tensile, and flexural strengths. Microstructural analyses revealed that the addition of WBGNPs improved the hydration process, increased gel density, and reduced porosity. From the obtained numerical results, the coefficient of determination value of 0.92 further confirms the model's predictive strength, demonstrating that the Random Forest algorithm can reliably estimate the compressive strength. The findings indicate that the concrete formulated with WTCP and WBGNPs not only meets diverse construction demands but also significantly contributes to environmental sustainability by reducing impacts on global warming and minimizing landfill usage. This study advocates for the strategic incorporation of WTCP and WBGNPs in concrete applications to promote environmentally sustainable construction practices. It is highly recommended that WTCP be utilized in sustainable binders as a replacement for OPC and natural aggregates to enhance it

---

* Corresponding authors.
** Corresponding author at: Guangzhou Institute of Energy Conversion, Chinese Academy of Sciences, Guangzhou, Guangdong 510640, China.
E-mail addresses: nur_hafizah@utm.my (N.H.A. Khalid), mohammad.baghban@ntnu.no (M.H. Baghban), ghasanfahim@gmail.com (G.F. Huseien).

strength and durable properties, reduce the environmental issues, costs, and the depletion of natural resources.

1. Introduction

In the construction industry, ordinary Portland cement (OPC) is the primary binder material used in concrete production, which is essential for modern infrastructure. The worldwide demand for OPC is set to escalate significantly, driven by global population growth and urbanization, particularly in developed countries such as China, the United States, and Japan. Studies predict that the worldwide demand for OPC will more than double by 2050 [1]. This increased demand comes with substantial environmental costs: it is associated with significant energy consumption, extensive use of raw materials, and large-scale emissions of greenhouse gases, nearly one ton of CO_2 per ton of cement produced, totaling approximately 1.5 billion tons of CO_2 annually [2]. Furthermore, the durability of concrete in aggressive environments and its overall lifecycle impact remain major concerns, given the material's susceptibility to various degradation processes.

The pursuit of sustainability in concrete production has led to significant research into the use of supplementary cementitious materials (SCMs) to reduce the environmental footprint of OPC [3–7]. Pozzolanic materials such as fly ash, silica fume, husk ash, and blast furnace slag have been widely studied and integrated into concrete mixes [8–10]. These SCMs react chemically with the calcium hydroxide released during the hydration of OPC to form additional calcium silicate hydrate (C-S-H), enhancing the strength and durability of concrete. Dhir et al. reported improvements in the fresh properties and compressive strength of concrete with the inclusion of these pozzolanic materials [11]. Ndahirwa et al. also observed enhanced durability and economic benefits from using SCMs, which are crucial for extending the service life of concrete structures and reducing maintenance costs [12]. Kumar et al. explored the incorporation of nano-silica with traditional SCMs like fly ash and silica fume [13]. Their findings reveal that nano-silica not only accelerates pozzolanic reactions but also enhances early strength gains and improves microstructural properties. This addresses the initial strength development delay often associated with SCM-enriched concrete, thus facilitating faster construction timelines. Additionally, this research highlighted that nano-enhanced SCMs significantly reduce permeability and increase resistance to chloride ingress, enhancing the durability of the concrete.

Despite the advantages, the application of SCMs has limitations [14]. The variability in the quality of these materials, depending on their source and processing, can affect the consistency and predictability of concrete properties. Furthermore, the availability of traditional SCMs like fly ash and slag is becoming increasingly constrained in many countries [15]. This scarcity is primarily due to the phased-out coal power stations that traditionally produce fly ash and the modernization of the iron industry, which is shifting towards electric arc furnaces that do not generate slag. Moreover, while SCMs can improve the long-term strength and durability of concrete, they may delay its initial strength development, posing challenges in fast-paced construction projects [16].

The integration of waste materials from industries such as ceramics has emerged as a promising area of study [17,18]. The ceramic industry generates significant amounts of waste, which when processed properly, can serve as a valuable pozzolanic material. Tile ceramic waste is particularly rich in silica and alumina, capable of participating in pozzolanic reactions that contribute to the formation of secondary C-S-H phases. Alsaif found that tile ceramic wastes could enhance the workability and mechanical properties of concrete when used as a partial replacement for OPC [19]. However, studies have noted that high percentages of ceramic waste can reduce early strength significantly, which limits its use in certain applications [20]. In a parallel study, Chen et al. investigated the use of recycled ceramic waste as an SCM, focusing on both environmental and mechanical performance enhancements in concrete [21]. Their results showed considerable reductions in CO_2 emissions due to the partial replacement of OPC with ceramic waste. Mechanically, the concrete exhibited improved durability and thermal stability, which were attributed to the pozzolanic activity of the ceramic waste. Although the inclusion of ceramic waste enhances mechanical properties and durability when used up to certain thresholds, studies like that of Le et al. reveal that higher levels of ceramic waste incorporation can significantly decrease workability and increase water permeability, limiting its practical application in construction [22]. This suggests a pressing need for research into formulations that maintain workability and control permeability while maximizing the use of ceramic waste.

Recent advancements in nanotechnology offer new opportunities to enhance the properties of concrete through the incorporation of nano-sized particles [23–25]. Nano-silica, in particular, has shown potential in significantly improving the hydration process [26], providing more compact microstructures [27], and enhancing early strength development [28]. The use of nano-silica in combination with ceramic wastes could potentially address the early strength limitations observed with larger-sized pozzolanic materials. Studies by Jiang et al. have demonstrated that the addition of nano-silica not only accelerates the hydration process but also significantly enhances the microstructural compactness of concrete [23]. Their findings reveal that nano-silica particles serve as nucleation sites that promote more rapid and uniform formation of calcium silicate hydrate (C-S-H) gel, leading to notable increases in early strength. This can be particularly beneficial in construction scenarios requiring rapid formwork removal or early application of load. Additionally, research conducted by Ramezanianpour et al. explores the synergistic effects of combining nano-silica with ceramic waste as supplementary cementitious materials [29]. Their study indicates that nano-silica effectively compensates for the slower reaction kinetics associated with the larger particle sizes of ceramic waste. The results show significant improvements in both the mechanical properties and durability of the concrete, with an evident increase in compressive strength observed within the initial seven days of curing. Moreover, the incorporation of nano-silica enhances pore refinement, yielding denser concrete with improved resistance to environmental degradation. However, while previous research demonstrates the benefits of nano-silica in overcoming early strength limitations and enhancing durability when combined with ceramic wastes, there remains a gap in fully understanding the optimal

proportions and processing methods that maximize these benefits without compromising the workability of concrete. Further exploration is needed to refine these nano-enhanced mixtures for broader practical applications in the construction industry.

Given this background, this study aims to systematically explore the synergistic effects of WTCAs, WTCP, and silica nanoparticles derived from waste bottle glass in concrete. By conducting a comprehensive analysis of mechanical properties and microstructural changes, this research will assess the feasibility of replacing significant portions of OPC with WTCP and WBGNPs, and natural aggregate with WTCAs aiming to develop high-performance concrete that meets stringent structural requirements and contributes to sustainability goals. This study will fill the critical gap in existing research by optimizing the particle size and reactivity of pozzolanic materials to enhance both early and long-term strength of concrete, thus supporting broader adoption in construction practices.

2. Methodology

2.1. Materials characterization

In this experiment, the WTCP and WBGNPs from industrial wastes are used as OPC replacements in a designed binder to prepare the concrete specimens (Fig. 1). The crushed ceramic is also utilized as fine and coarse natural aggregate replacement. The chemical compositions, physical characteristics, morphology, and microstructure of used materials are assessed. To measure the physical properties of used materials such as specific gravity, surface area fineness, median particle size, Pycnometer, Brunauer Emmett Teller (BET), and Particle size analysis (PSA) tests were conducted. For the OPC, the physical properties show that the utilized cement has a dark grey color, 3.15 specific gravity, 3995 cm^2/g surface area fineness, 16.4 μm median particle sizes, and 97 % of particles passed through a 45μm wet sieve. The used cement achieved the essential chemical requirements for ASTM Type I cement, as stated by ASTM C150 [30]. The chemical compositions of the OPC are described in Table 1. In general, the primary chemical components of OPC are calcium oxide (67 %) and silica oxide (17 %). The high content of CaO in OPC (67 %) is responsible for higher hydration reaction and higher strength at an early age [31], as opposed to prepared ceramic powder (0.02 %).

The median of prepared WTCP particles was found to be 17.1 μm. Furthermore, the particle size of 97 % of ceramic powder is less than 45 μm. The particle size of ceramic powder was in line with OPC after 6 hrs of grinding. Thus, these results fulfilled the pozzolanic

**Fig. 1.** Raw materials utilized to prepare the sustainable concrete.

Table 1

The chemical compositions of cement, tile ceramic powder, and glass bottle nanoparticles used in the XRF test by element weight %.

Chemical Compositions	OPC	WTCP	WBGNPs
Silica oxide, SiO_2	17.60	71.7	69.14
Aluminium oxide, Al_2O_3	4.54	13.9	13.86
Sodium oxide, Na_2O	2.49	13.21	8.57
Iron oxide, Fe_2O_3	3.35	0.37	0.24
Calcium oxide, CaO	67.84	0.02	3.16
Magnesium oxide, MgO	2.18	0.64	0.68
Potassium oxide, K_2O	0.27	0.03	0.01
Loss on ignition, LOI	1.73	0.13	0.16

requirement of ASTM C618 [32] of 66 % passing 45 μm. In term of physical properties of WTCP, the prepared powder was light gray, 16.4 m^2/g, and 3.06 specific gravity. The particular gravity directly affected the surface area and remained lower than the OPC material. X-ray fluorescence (XRF) spectroscopy test (machine brand of Perkin Elmer, FL 6500) was used to detect the chemical compositions of utilized materials, as summarized in Table 1. The principal oxide compositions were silica and aluminum in the presence of 85.6 % ceramics. Notably, the silicate, aluminium, and calcium oxide level played a significant role in the specimens' synthesis by forming the C-A-S-H and C-S-H in the hydration process. The sodium oxide (Na_2O) content was observed at a high ratio (13.2 %) in the ceramic chemical composite. It is known that Na_2O can strongly affect the hydration process. The Loss on Ignition (LOI) contents were meager in WTCP, consistent with the ASTM C618 standard.

The results obtained from the tested WBGNPs found the median particle size, specific surface area, and specific gravity of 80 nm, 206 m^2/g, and 1.02, respectively. Likewise, the nanoparticle of glass powder's effect on the surface area test presented a very high value compared to OPC and prepared ceramic powder. Table 1 depicts the chemical composition of silica nanoparticles from WBGNPs obtained using X-ray fluorescence spectroscopy. The primary oxide elements were aluminum and silica, 83 % in WBGNPs. Besides, WBGNPs exhibited reduced LOI values, which align with the standards outlined in ASTM C618.

The crushed granite stone is used as the coarse aggregate, free from harmful materials such as organic matter, grass and leaves, dry mud, silt, and oil. The aggregates are kept under saturated surface dry (SSD) conditions to ensure their insignificant effect on the amount of free water in the mix design. As shown in Fig. 2, the sieve analysis is conducted for coarse aggregate grading according to ASTM C136 [33]. Furthermore, the coarse aggregate tested for the specific gravity was 2.67 under the SSD conditions, water absorption was 1.2 % (according to ASTM C127 [34]), and maximum particle size was 10 mm. For alternative wastes, ceramic coarse aggregates, the crushed ceramic with a maximum size of 10 mm and according to ASTM C33 [35] were utilized in this study to replace
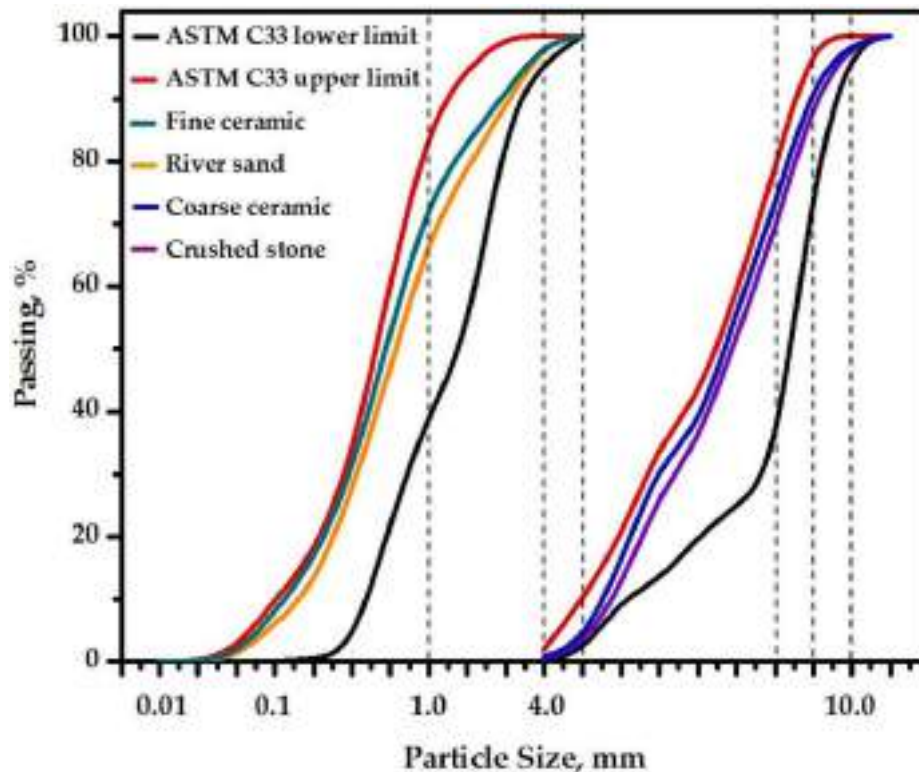
Fig. 2. Sieving analysis of river sand, crushed stone, fine and coarse ceramic aggregates.

the natural aggregates.

In preparing the concrete specimens, the river sand is used as the fine aggregates acquired in compliance with the ASTM C33 requirements. To achieve an acceptable water-cement ratio, the sand is maintained to SSD, as stipulated in ACI-219 before use. Sieve analysis is conducted to determine the grading of fine aggregate according to ASTM C136. Furthermore, the natural fine aggregate's absorption capacity and specific gravity are tested under SSD conditions (ASTM C128 [36]). The sand is well-graded, with a fineness modulus of 2.8. Thus, the fineness modulus value of fine aggregate shows that it is suitable for use in the concrete mixture. With a line of ASTM C33, the ceramic wastes were crushed and sieved to be ideal as fine aggregates to replace the river sand in preparing the proposed concretes.

2.2. Mix design

The development of sustainable high-performance concrete incorporating WTCAs, WTCP, and WBGNPs encompasses five distinct phases, as depicted in Fig. 3. The control mix, consisting solely of natural aggregates and OPC, targeted a compressive strength exceeding 30 MPa after 28 days of curing, suitable for various structural applications. In the initial phase, trial mixtures assessed the suitability of WTCAs as replacements for fine and coarse aggregates. Table 2 details the mix designs employing WTCAs as replacements. The criteria adopted to select the optimum mixture in each phase of these experiments were based on achieving the highest compressive strength after 28 days of curing for phases 1, 3, and 4. However, for phase 2, the mixture with the highest amount of WTCPs that achieved a compressive strength of $\geq$20 MPa after 28 days was considered optimal. This mixture was then modified with nanoparticles to increase its strength to 30 MPa after 28 days of curing.

The second phase focused on the influence of high-volume WTCP as a replacement for OPC, analyzing compressive strength at both 7 and 28 days of curing, see Table 2. Control specimens comprised 420 kg/m^3 OPC, 816 kg/m^3 fine ceramic aggregate, and 894 kg/m^3 coarse ceramic aggregate, with a water-to-cement ratio (w/c) of 0.55. Subsequent mixes progressively replaced OPC with 10–70 % WTCP, maintaining constant aggregate and water volumes. The optimal mix from this phase was determined by the highest WTCP volume that still achieved at least 20 MPa compressive strength at 28 days.

Phase 3 investigated the effects of varying water-cement ratios and superplasticizer (SP) content on the compressive strength of high-volume ceramic concrete, see Table 2. Keeping the binary binder and aggregate content constant, water-cement ratios of 0.42, 0.48, and 0.55, along with SP levels of 1 %, 1.5 %, and 2 %, were tested. The mix yielding the highest strength at 28 days was selected for further development.

Phases 4 and 5 (as shown in Table 3) refined the mix design for sustainable high-volume ceramic concrete, incorporating silica nanoparticles from WBGNPs to enhance hydration and microstructure. The final mix consisted of 252 kg/m^3 WTCPs, 168 kg/m^3 OPC, with set ratios of aggregates, water-cement, and SP. WBGNPs were added at 2–10 % of the total binder content. The effectiveness of these additions was evaluated through comprehensive testing, including compressive, splitting tensile, and flexural strength tests, along with X-ray Diffraction (XRD), Differential Thermogravimetry (DTG), Field Emission Scanning Electron Microscopy - Energy Dispersive X-ray (FESEM-EDX), and Atomic Force Microscopy (AFM) analyses.
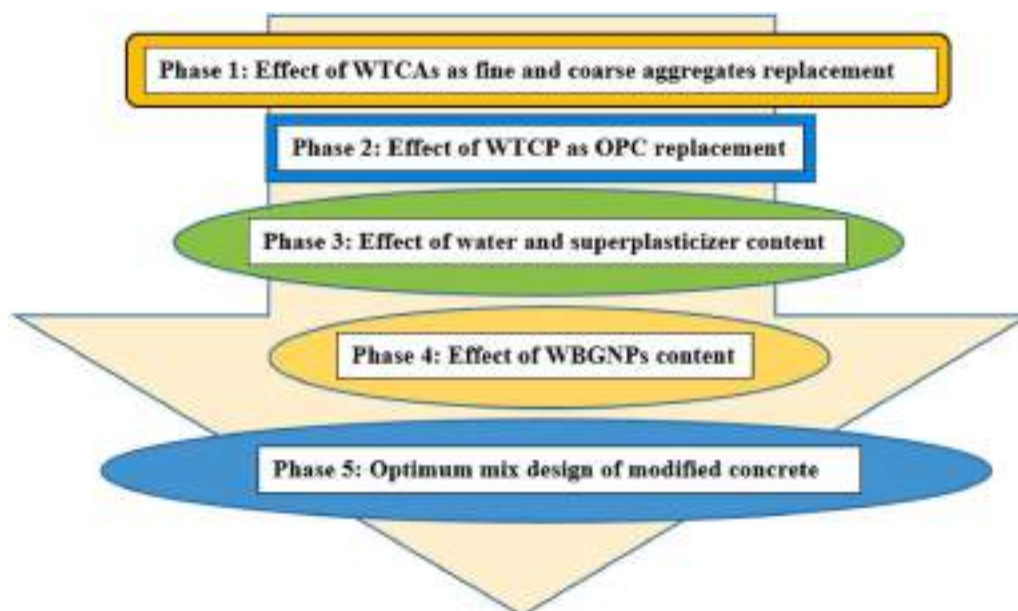

Fig. 3. Sustainable concrete' mixtures procedures.

Table 2

Mix design of wastes ceramic as fine and coarse aggregates replacement, kg/m^3.

Phase	Mix code	Binder, kg/m^3		Natural aggregates		WTCAs		W/C	SP, %
		OPC	WTCP	Fine	Coarse	Fine	Coarse		
Phase (1)	WCA0	420	0	816	894	0	0	0.55	0
	WCA25	420	0	612	670	204	224	0.55	0
	WCA50	420	0	408	447	408	447	0.55	0
	WCA75	420	0	204	224	612	670	0.55	0
	WCA100	420	0	0	0	816	894	0.55	0
Phase (2)	WTCP0	420	0	0	0	816	894	0.55	0
	WTCP10	378	42	0	0	816	894	0.55	0
	WTCP20	336	84	0	0	816	894	0.55	0
	WTCP30	294	126	0	0	816	894	0.55	0
	WTCP40	252	168	0	0	816	894	0.55	0
	WTCP50	210	210	0	0	816	894	0.55	0
	WTCP60	168	252	0	0	816	894	0.55	0
	WTCP70	126	294	0	0	816	894	0.55	0
Phase (3)	H42–1.0	168	252	0	0	816	894	0.42	1.0
	H42–1.5	168	252	0	0	816	894	0.42	1.5
	H42–2.0	168	252	0	0	816	894	0.42	2.0
	H48–1.0	168	252	0	0	816	894	0.48	1.0
	H48–1.5	168	252	0	0	816	894	0.48	1.5
	H48–2.0	168	252	0	0	816	894	0.48	2.0
	H55–1.0	168	252	0	0	816	894	0.55	1.0
	H55–1.5	168	252	0	0	816	894	0.55	1.5
	H55–2.0	168	252	0	0	816	894	0.55	2.0

Table 3

Mix design of sustainable concrete containing silica nanoparticles, kg/m^3 (phases 4 and 5).

Mix code	Binder, kg/m^3			WTCA, kg/m^3		W/C	SP, %
	OPC	WTCPs	WBGNPs	Fine	Coarse		
OPC	420	0	0	816	894	0.48	1.5
60WCP	168	252	0	816	894	0.48	1.5
2NPs	168	252	8.4	816	894	0.48	1.5
4NPs	168	252	16.8	816	894	0.48	1.5
6NPs	168	252	25.2	816	894	0.48	1.5
8NPs	168	252	33.6	816	894	0.48	1.5
10NPs	168	252	42	816	894	0.48	1.5

2.3. Specimens preparation and test procedure

In mixing the proposed binder, OPC, WTCP, and WBGNPs blended for 3 minutes using a blender machine to achieve the homogenous ternary blended binders. A drum mixer with a capacity of 0.2 m^3 was used for mixing the materials to produce uniform concrete. Firstly, 50 % of fine and coarse aggregates were mixed for 2 minutes then the remaining amount of fine and coarse aggregates (50 %) added and mixed for another 3 minutes in dry condition of materials. Then, the ternary blended binders of OPC-WTCP-WGBNPs were added. Total materials (binders, fine and coarse aggregates) were mixed in a dry condition for another 5 minutes before being activated with the water and SP solution. Finally, the activated mixtures were mixed for another 4 minutes before evaluating the slump value and poured into the prepared steel moulds following the ASTM C579–18 [37]. According to ASTM C143 [38], the workability of fresh concrete is evaluated using a slump test. For the preparation of concrete specimens, three types of molds were utilized: cubical (100 mm × 100 mm × 100 mm), cylindrical with a diameter of 100 mm and depth of 200 mm, and beam (500 mm × 100 mm × 100 mm), following the standards of BS 1881–108, 1881–109, and BS 1881–110, respectively. The molds were thoroughly cleaned to ensure no residue from previous uses remained. The concrete mix was then poured into the molds in layers, each compacted using a vibration table to minimize air entrapment. The surface of each mold was subsequently smoothed using a plasterer's float. Then, the specimens were left for 24 hours in lab condition (temperature of 26°C ± 1.5/ relative humidity more than 75 %) before being de-moulded and cured in water for 7 days.

Mechanical properties such as compressive, tensile, and flexural strengths were evaluated in accordance with ASTM standards C109/109 M [39], C496/C496M-11 [40], and C78, respectively. Specimens were cured for set durations of 3, 7, 28, 56, and 90 days to assess compressive strength. For each age, three specimens were tested and the average reading was considered. For microstructural analysis, pastes of OPC (control sample), binary blended of OPC-WTCP, and ternary blended of OPC-WTCP-WGBNPs were prepared for this purpose, and the specimens evaluated after 7 and 28 days of curing ages. Several microstructure tests were conducted such as FESEM, EDX, TGA, DTG, AFM, and XRD using different machines and techniques. For the FESEM and EDX tests, the selected samples were mounted, dried, and coated to enhance conductivity before imaging. To conduct this test, specimens with a maximum size of

1.5 mm were dried using an infrared radiation process then the specimens were coated with a gold layer using a blazer sputtering coater. Recordings of 20 kV with 1000× magnification were used for the patterns. For the XRD, TGA, and DTG tests, samples were prepared by grinding into fine powder. Following to the procedure recommended by Alva et al. [41], the paste samples were prepared and the AFM test was conducted after 7 and 28 days of curing age.

3. Results and discussion

3.1. Workability

The effect of high-volume waste ceramic powder and nanoparticles of silica on fresh concrete workability were evaluated and the obtained results are presented in Fig. 4. The results indicated that the inclusion 60 % of wastes ceramic powder as ordinary Portland cement (OPC) replacement significantly led to reduce the workability of prepared concrete the drop the slump value from 190 mm to 154 mm. The pores and irregular shapes of ceramic particles led to increase the demand of water which led to loss the workability of proposed concrete. Likewise, the results shown that the inclusion of nanoparticles of silica in the matrix of high ceramic cement slightly led to loss the workability of concrete. It's found with the rising content of silica nanoparticles from 0 % to 2, 4, 6, 8, and 10 % the slump value of concrete dropped from 154 mm to 149, 142, 138, 132, and 128 mm, respectively. it's well known the reduction in workability of proposed concrete is attributed to a high specific area of nanoparticles which resulted high demand of water, increased the viscosity of concrete, and dropped the slump values [42,43].

3.2. Compressive strength

The effect of WTCAs (as fine and coarse aggregates replacement), WTCP (as OPC replacement), W/C, and SP on 7 and 28 days' compressive strength were evaluated and the obtained results are presented in Fig. 5. Fig. 5(a) demonstrates the impact of replacing river sand and crushed stone with WTCAs on the compressive strength development of the proposed concrete. At both 7 and 28 days of curing, it's observed that the inclusion of WTCAs in the concrete matrix slightly enhances the strength performance. At 7 days, compressive strength values were recorded at 26.4, 24.9, 25.4, and 27.3 MPa for 25 %, 50 %, 75 %, and 100 % replacement levels, respectively, compared to a control strength of 25.9 MPa. Similarly, at 28 days, the replacements resulted in strengths of 35.2, 34.7, 35.6, and 36.5 MPa, with the control mix at 35.4 MPa. The 100 % replacement level yielded the highest compressive strength at both testing ages, leading to its selection for further experimentation. Compared to the fine and coarse natural aggregates, the surface roughness and irregular shape of WTCAs significantly affect on the interlock with the cement paste and result greater bond zone and higher strength performance [44,45].

Fig. 5(b) shows the impact of varying WTCP contents as OPC replacements on the compressive strength of concrete after 7 and 28
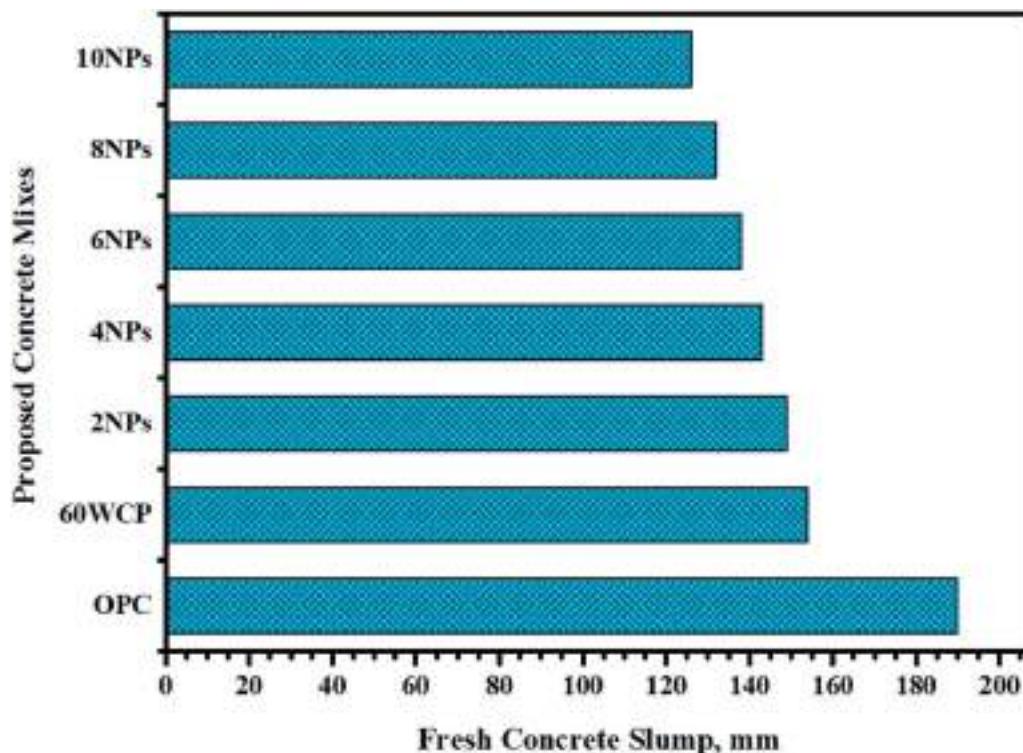

Fig. 4. Workability of proposed concrete incorporating high-volume ceramic and waste bottle glass nanoparticles.
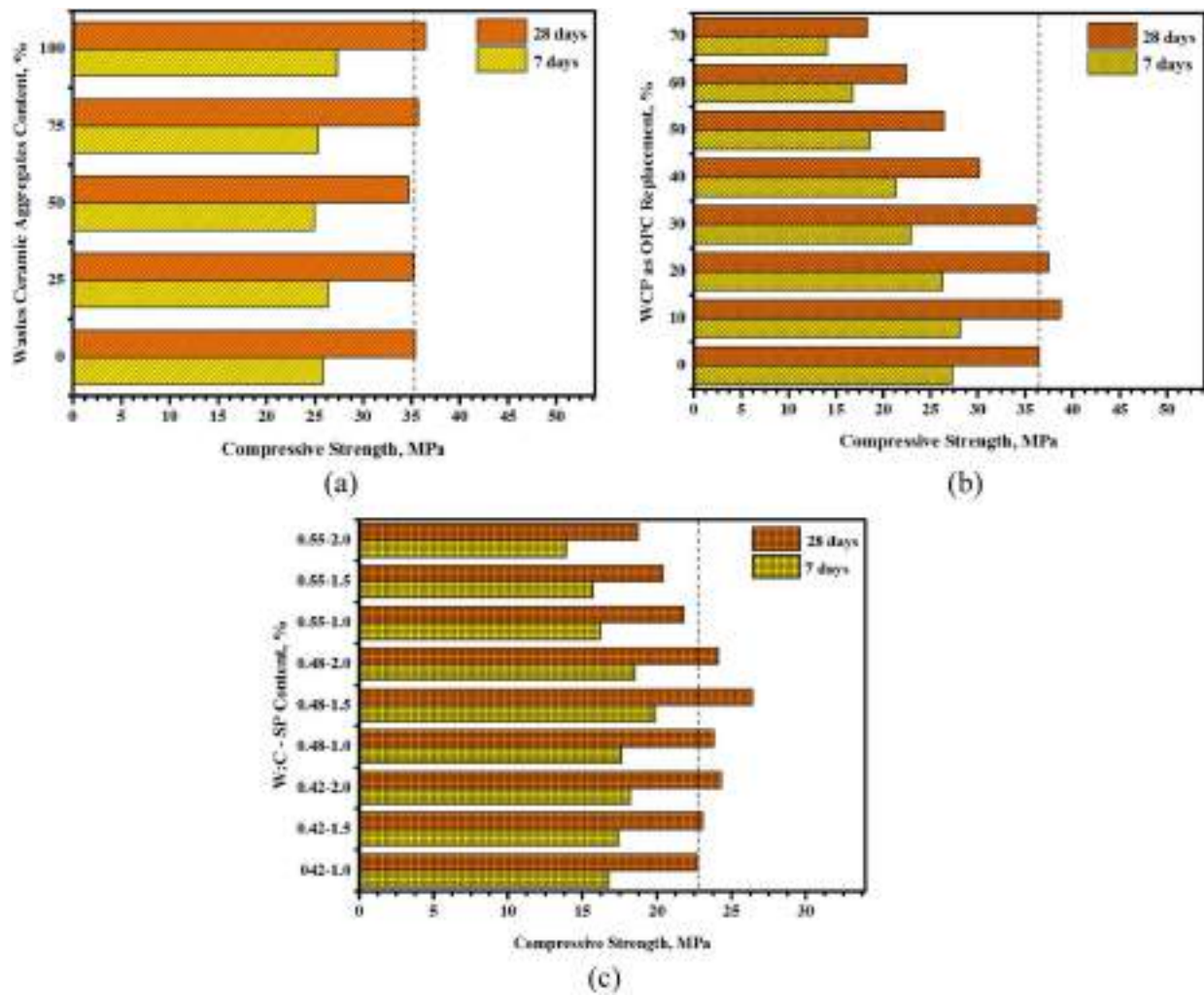
Fig. 5. The effect of (a) WTCA as a fine and coarse aggregate replacement, (b) WTCP as OPC replacement, (C) W/C ratio and SP content.

days of curing age. Initially, 10 % WTCP replacement enhances strength from 27.3 MPa to 28.1 MPa at 7 days and from 36.5 MPa to 38.7 MPa at 28 days. The enhancement of compressive strength of the proposed concrete was attributed to the increasing in content of SiO_2, and Al_2O_3 which were reactive with $Ca(OH)_2$ and formulated more C-(A)-S-H gels [46]. The increment in dense gels production significantly can improve the bond zone between the modified cement and aggregates' surface and show higher strength performance [47]. However, further increases in WTCP lead to a decline in early strength, with 20–70 % replacements resulting in progressively lower strengths. At 28 days, strengths up to 30 % replacement are comparable to the control, but higher replacements continue to show reduced strength. This pattern is attributed to the reduced presence of CaO, C_2S, and C_3S, affecting early hydration but improving over time due to the pozzolanic reaction's delayed efficacy [46,48]. The highest drop in strength with a high amount of WTCP ($\geq$50 %) was attributed to high silica concentration which directly restricted the C-(A)-S-H gels formulation and led to lower strength performance [49]. A mix with 60 % WTCP met the target strength of 20 MPa at 28 days and was advanced for further experimentation.

Fig. 5(c) highlights the impact of varying water content and superplasticizer levels on the compressive strength of concrete at 7 and 28 days. An increase in curing age consistently enhanced compressive strength across all mixtures. Notably, the mixture with a 0.48 water-cement ratio and 1.5 % SP outperformed others, reaching 19.9 MPa at 7 days and 26.4 MPa at 28 days, significantly higher than the control sample's 16.8 MPa and 22.5 MPa, respectively. This mixture was selected as the optimum for further development in the sustainable high-volume ceramic concrete project. It's well known the higher or lower content of water and SP directly affect in cement hydration process. The higher content leads to more liquids not used in hydration process of cement creates more voids in structure of concrete, weakening its overall strength performance [50,51]. However, the lower content typically leads to an uncompleted hydration process with more CaO, SiO_2, and Al_2O_3 non-reactive [52,53].

Fig. 6 displays the impact of varying contents of silica nanoparticles from WBGNPs on the compressive strength of concrete over time. The addition of WBGNPs, particularly 2, 4, 6, 8, and 10 %, to a high-volume WTCP mix (60 %) consistently improved early and late-age compressive strengths. For all concrete specimens, the compressive strength tends to increase with increasing curing ages. At an early age (3 days), the results showed that the inclusion of 2, 4, 6, 8, and 10 % of WBGNPs to the matrix of high-volume ceramic (60 %) led to improved compressive strength from 10.6 MPa to 14.2, 16.8, 15.9, 14.7 and 12.9 MPa, respectively. However, most the
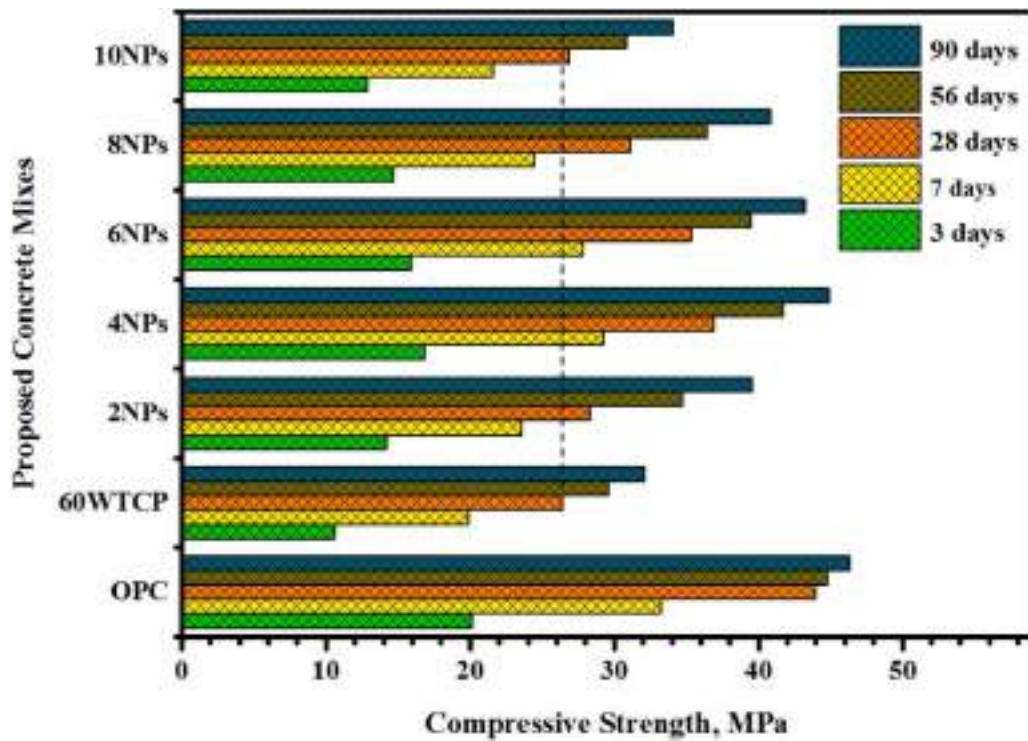
Fig. 6. Effect of WBGNPs content on compressive strength development of proposed concrete at various curing ages (3, 7, 28, 56 and 90 days).

specimens prepared with various level of WBGNPs shown lower performance compared to 100 % OPC mixture which was achieved compressive strength closed to 20.1 MPa. A similar trend of results for the specimens evaluated after 7 days of curing age and the compressive strength slightly increased from 19.9 MPa to 23.6, 29.2, 27.8, 24.4, and 21.6 MPa with the inclusion of 2, 4, 6, 8, and 10 % of WBGNPs to the matrix of high volume ceramic. At 28 days of age, the tested specimens containing 2, 4, 6, 8, and 10 % of nano-particles achieved strength of 28.3, 36.9, 35.3, 31.1, and 26.9 MPa which is higher than high ceramic mixture compressive strength (26.4 MPa). At late age (56 and 90 days), the specimens prepared with 4 and 6 % of WBGNPs modified high volume ceramic matrix achieved closed strength to 100 % OPC mixture and recorded compressive strength of 44.9 and 43.2 MPa compared to 46.3 MPa, respectively. For instance, at 28 days, the inclusion of 4 % WBGNPs led to the highest increase, enhancing strength by over 38 % compared to the high ceramic mixture alone. This enhancement is attributed to the nanoscale particles accelerating hydration, improving gel density, reducing porosity, and refining the microstructure of the concrete [54–57]. It's summary that the incorporation of nanomaterials into modified concrete contributes to filling and microaggregate effects, promoting the formation of cementitious materials and resulting in a denser matrix. Additionally, due to its reactivity, silica nanoparticles can react with calcium hydroxide to
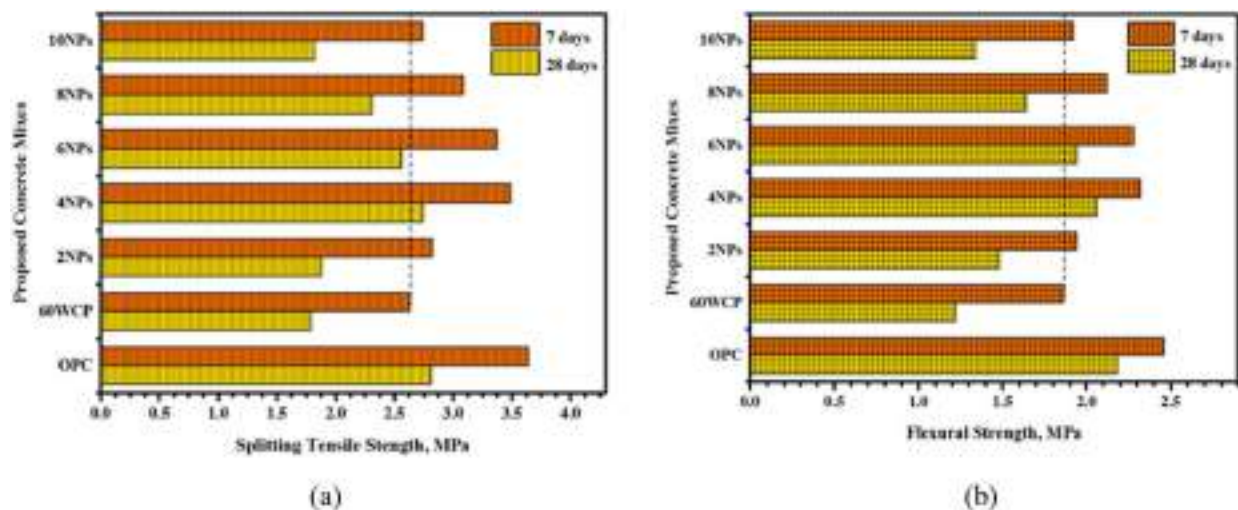

Fig. 7. The effect of WBGNPs content on (a) splitting tensile strength and (b) Flexural strength development of specimens with high WTCP content at 7 and 28 days of curing age.

produce more dense gels such as C-S-H, thus increasing strength, while silica nanoparticles can react with calcium hydroxide to form additional C-(A)-S-H [58,59]. Nanomaterials can interact with Tricalcium aluminate, a principal component of cement clinker, to create calcium carbonate aluminates [60,61]. An optimal quantity of nanomaterials can significantly enhance the compressive strength of the proposed concrete.

3.3. Splitting tensile and flexural strength

Fig. 7 displays the results of splitting tensile and flexural strength of concrete specimens prepared with high-volume ceramic powder (60 %) as OPC replacement and incorporating WBGNPs. For all evaluated specimens, it's observed the strength value trend to increase with increasing curing age from 7 to 28 days. Fig. 7(a) illustrates the effects of incorporating WBGNPs into high-volume ceramic concrete on its splitting tensile strength at different curing ages. The addition of 2, 4, 6, 8, and 10 % WBGNPs significantly enhances the tensile strength, particularly evident at 28 days with a peak strength of 3.49 MPa for the 4 % inclusion, closely approaching the performance of 100 % OPC concrete at 3.64 MPa. This improvement in tensile strength is attributed to the nano-particles enhancing the microstructural bonding within the concrete matrix [62,63], leading to better performance over time compared to the high-volume ceramic matrix without nanoparticles.

Fig. 7(b) displays the flexural strength of concrete beams incorporating WTCP and WBGNPs at various percentages. With increased curing time, all specimens showed enhanced flexural strength. At 7 days of age, the inclusion of 2, 4, 6, 8, and 10 % of WBGNPs in the matrix led to an increase in the splitting tensile strength from 1.79 MPa to 1.88, 2.74, 2.56, 2.31, and 1.82 MPa, respectively. However, most the modified concrete specimens shown lower strength performance compared to 100 % OPC specimens which was recorded 2.81 MPa. Notably, at 28 days, the addition of 4 % WBGNPs achieved a peak flexural strength of 2.32 MPa, closely approaching that of 100 % OPC concrete at 2.46 MPa. This improvement is linked to the nanoparticles' role in enhancing hydration and gel formation, which strengthens the bond between the modified paste and aggregate surfaces [64–66]. As shown in Fig. 8, the linear regression method was applied to correlate the experimental data of proposed concrete' compressive strength vs splitting tensile and flexural strengths. The R^2 values ranged between 0.8781 – and 0.8794 for all specimens and signified good confidence in the correlation

3.4. Failure mood

Fig. 9 illustrates the failure modes of cubic specimens containing WTCPs and WBGNPs under static load. Increasing WTCP content as OPC replacement up to 20 % led to a reduction in compressive strength (Fig. 5(b)). Specimens with high ceramic content (Fig. 9(b)) maintained better structural integrity under ultimate load conditions compared to OPC concrete (Fig. 9(a)), which exhibited more brittle fracture and chipping. The addition of 4 % silica nanoparticles improved geometrical integrity and reduced the appearance of vertical cracks (Fig. 9(c)), enhancing the anti-cracking performance significantly compared to standard OPC concretes.
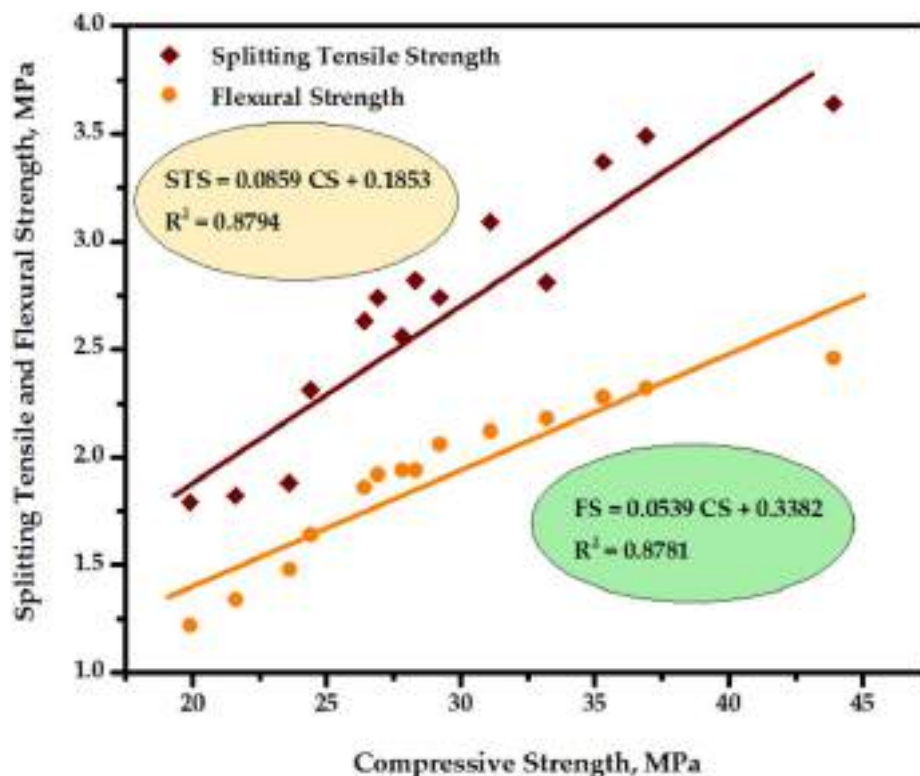

Fig. 8. Relationship between the modified concrete compressive (CS), splitting tensile (STS), and flexural strengths (FS).
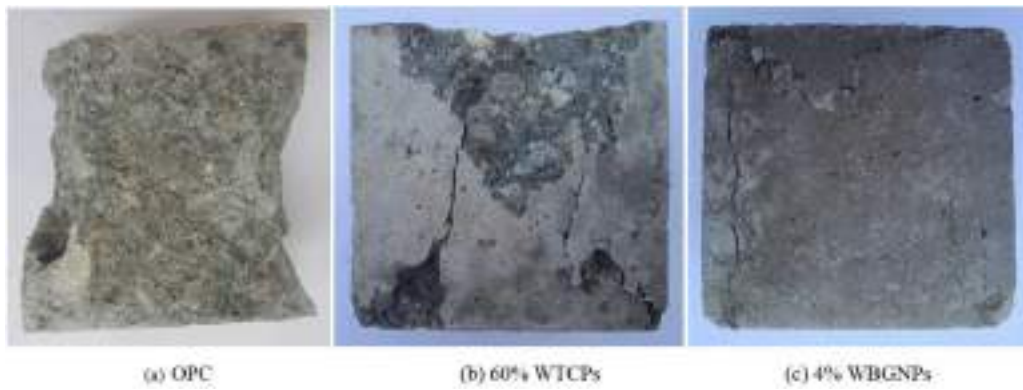
Fig. 9. Failure modes of the prepared concrete.

4. Microstructure analysis

4.1. Field emission scanning electron microscopy analysis

Field emission scanning electron microscopy (FESEM) and energy dispersive X-ray spectroscopy (EDX) analyses were conducted on concrete specimens containing 100 % OPC and those modified with 60 % WTCP and 4 % silica nanoparticles from WBGNPs. The results, illustrated in Figs. 10 to 12, reveal distinct differences in the microstructural development between the specimens over curing periods of 7 and 28 days.

Fig. 10 illustrates the FESEM images of OPC concrete at different stages of curing, with panel (a) showing the microstructure at 7 days and panel (d) depicting the more developed microstructure at 28 days, highlighting the progressive formation of hydration products such as calcium hydroxide (Ca(OH)$_2$), calcium-silicate-hydrate (C-S-H), calcium-aluminate-silicate-hydrate (C-A-S-H) and calcium carbonate (CaCO$_3$) [67–70].

For the 100 % OPC specimens, early age analysis (7 days) displayed a predominance of calcium hydroxide needles, as shown in Fig. 10 (a), whereas at 28 days, a denser gel structure predominantly composed of C-S-H and C-A-S-H was observed (Fig. 10 (d)). This transformation is linked to an increase in compressive strength from 33.2 MPa to 43.9 MPa, underscoring the role of hydration products in the development of mechanical properties [67,68].

Fig. 10 presents the FESEM images demonstrating the microstructural changes in concrete with 60 % WTCP as OPC replacement, where panel (b) captures the state at 7 days and panel (e) at 28 days, illustrating how WTCP inclusion contributes to the evolution and densification of the microstructure over time [22].
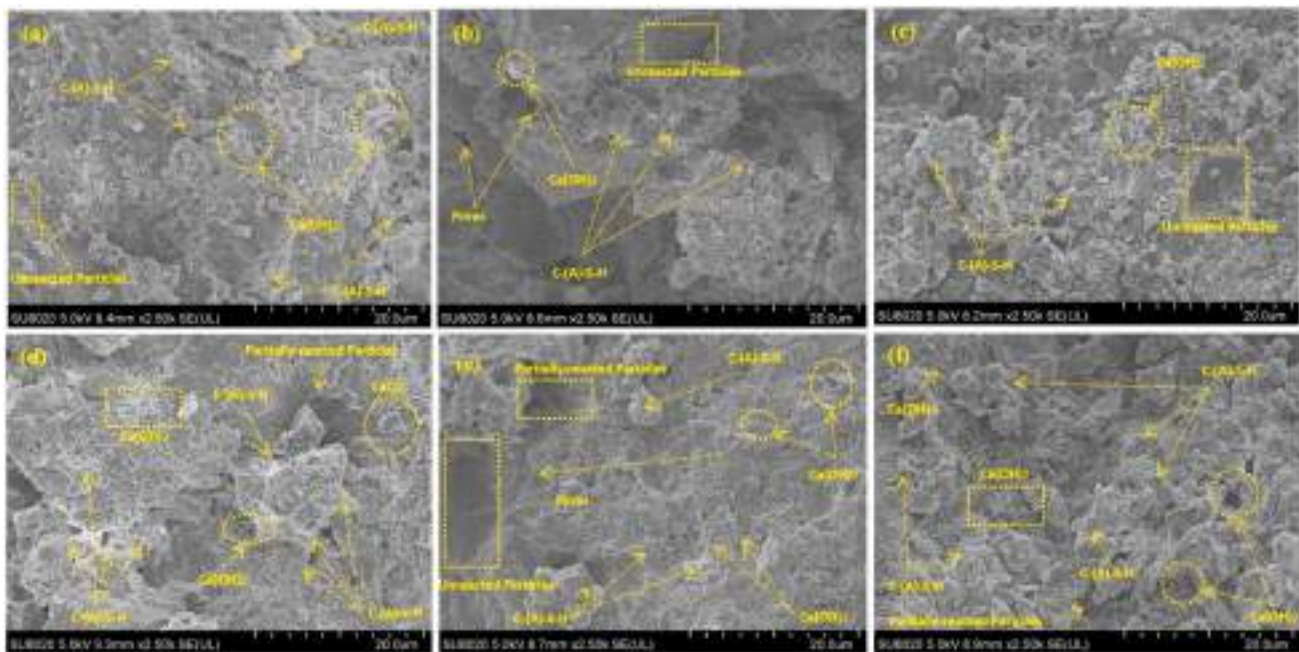

Fig. 10. FESEM of modified concrete. FESEM results for modified specimens at 7 days having binder (a) OPC (b) 60 % WTCP (c) 4 % WBGNPs and at 28 days of (d) OPC (e) 60 % WTCP (f) 4 % WBGNPs.
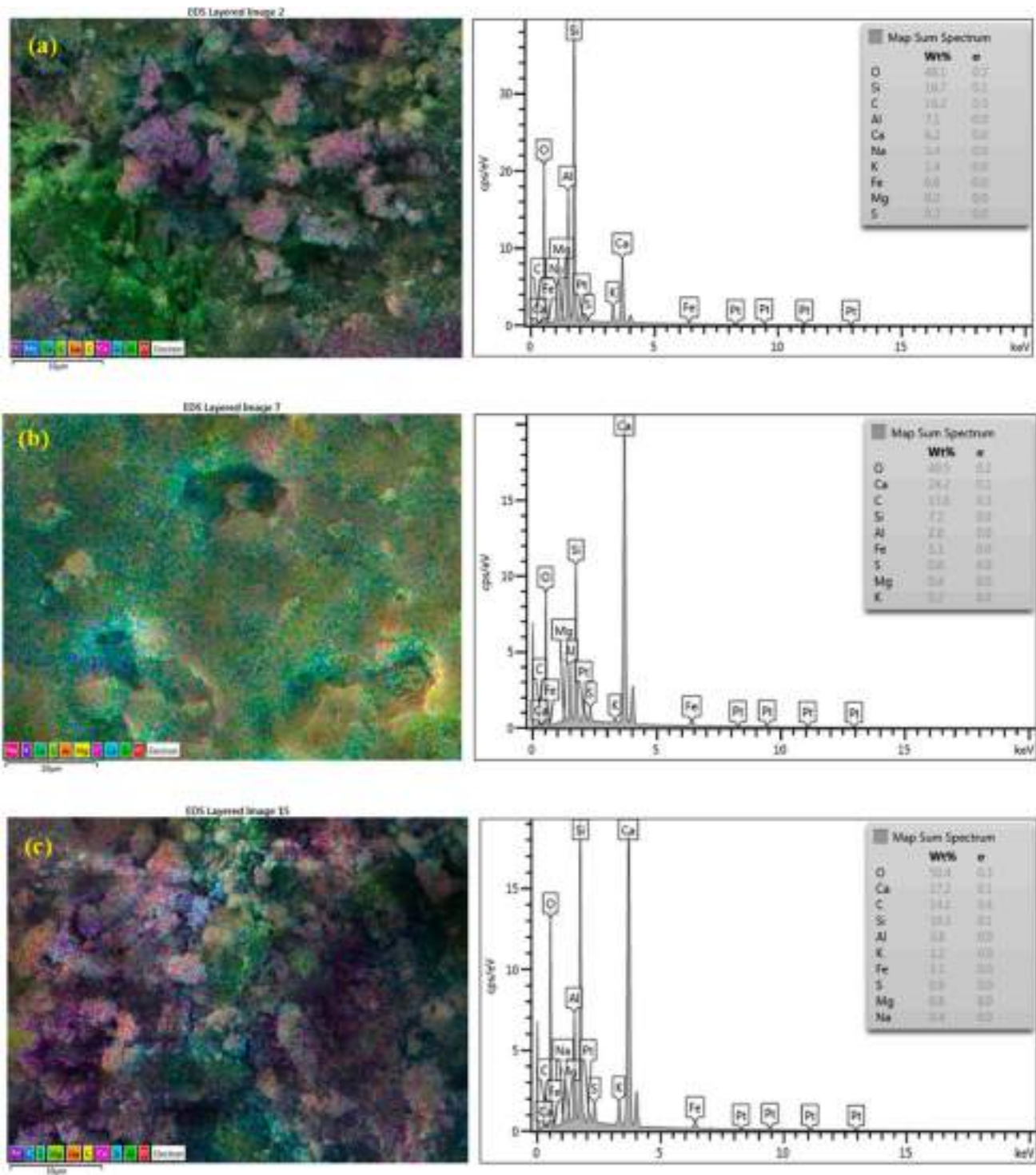
Fig. 11. EDX analysis results at age of 7 days (a) OPC (b) 60 % WTCP (c) 4 % WBGNPs.

A similar trend of increasing dense gel formation from 7 to 28 days was observed in specimens with 60 % WCP as OPC replacement, as depicted in EDX results (Figs. 11 and 12). Fig. 11 (b) shows that replacing OPC with 60 % of WTCP resulted in a higher presence of partially and non-reactive particles, accompanied by increased pores and non-homogeneous structures [71]. This microstructural alteration significantly reduced the mechanical performance and bond strength between the paste and aggregate, leading to lower overall strength in the modified concrete.

Fig. 10 displays the FESEM images of the modified binder containing 4 % WBGNPs at different curing times, with panel (c) showing the microstructural development at 7 days and panel (f) at 28 days, demonstrating the progressive improvement in matrix densification facilitated by the nanoparticle inclusion [72].
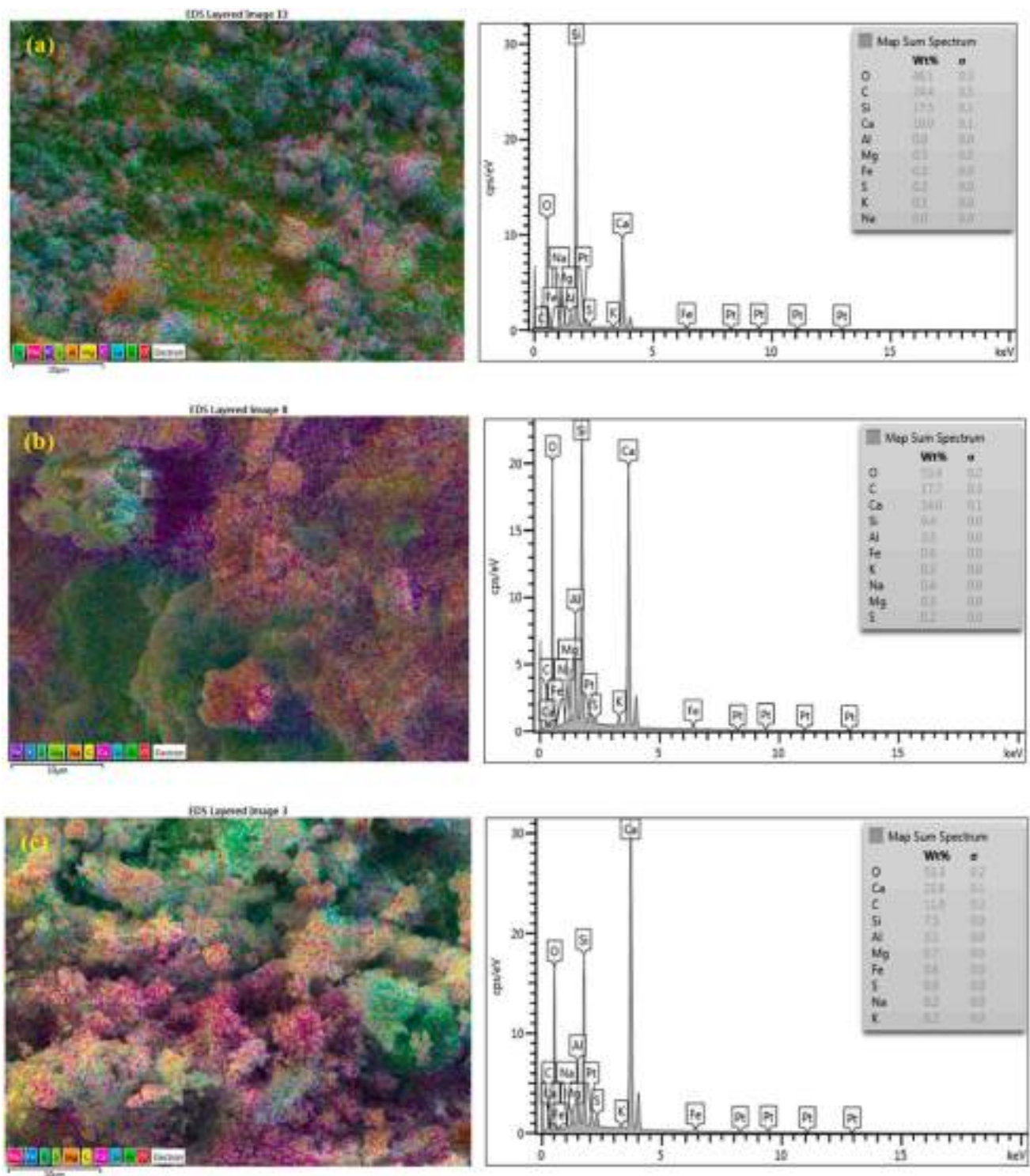
Fig. 12. EDX analysis results at the age of 28 days (a) OPC (b) 60 % WTCP (c) 4 % WBGNPs.

The inclusion of WBGNPs significantly enhanced the hydration process, leading to increased silica dissolution and more robust gel formation, as shown in Fig. 10 (f), 11 (c), and 12 (c). This improvement in the microstructure of the paste notably enhanced the bond strength with the aggregate surface [73–75] and resulted in superior strength performance compared to specimens prepared with 60 % high-volume WTCP.

4.2. Differential thermogravimetry analysis

DTG analysis, incorporating thermogravimetric analysis (TGA) and derivative thermogravimetry (DTG) tests, was conducted to

assess the weight loss and the formulation of $Ca(OH)_2$, $CaCO_3$, and C-S-H gels across various specimens. These tests were performed at 7 and 28 days on four different specimen types: 100 % OPC, 60 % WTCP, and concrete containing 4 % and 6 % nanoparticles from WBGNPs. The results are detailed in Fig. 13.

Fig. 13 displays the TGA-DTG analysis of OPC specimens, revealing the thermal behavior and decomposition profiles at different curing times; panel (a) represents results at 7 days and panel (d) at 28 days, illustrating significant changes in material properties over time. Similarly, Fig. 13(b) shows the TGA-DTG results for specimens with 60 % WTCP as OPC replacement, noting a marked reduction in the formation of $Ca(OH)_2$ and C-S-H gels at both 7 and 28 days [76], highlighting the impact of high WTCP content on microstructural development. Additionally, Fig. 13(c) presents the analysis of specimens enhanced with 4 % WBGNPs; the inclusion of nanoparticles substantially improved gel formulation and increased $Ca(OH)_2$ content, which significantly contributed to higher compressive strength results at 28 days—rising from 26.4 MPa in the high ceramic mix to 36.9 and 35.3 MPa, thereby demonstrating superior strength performance due to improved microstructural properties [63,77]."

The percentage weight loss of the OPC, 60 % WTCP, and 4 % WBGNPs' pastes samples were calculated based on the TGA and DTA obtained results. The percentages of Portlandite and dense gels were computed by using Eqs. 1 and 2, respectively.

$$\text{Portlandite, \% = WLP (\%)} \times [\text{MWP / MWW}] \tag{1}$$

$$\text{Dense gels, \% = LST} - \text{LSP} - \text{LSC} \tag{2}$$

where WLP is the weight loss due to calcium hydroxide dehydration at the temperature of $400 - 550\,°C$, MWP is the molecular weight of calcium hydroxide ($74\ \text{g.mol}^{-1}$), and MWW is the molecular weight of water ($18\ \text{g.mol}^{-1}$). LST: is the total loss in weight at $900\,°C$; LSP: is the loss at dehydration of calcium hydroxide; LSC: Is the loss at dehydration of carbonate calcium (600–$750\,°C$).

It's clear from the analysis results presented in Table 4 can be seen that the inclusion of 60 % of WTCP as OPC replacement affects on hydration process and formulation of Portlandite and dense gels which led to lower strength performance (as presented in Fig. 6). However, the inclusion 4 % of nanoparticles in the proposed binder significantly improved the hydration process and led to more Portlandite and dense gel formulation which resulted in a significant increment in strength development at both ages (7 and 28 days).

4.3. Atomic force microscopy analysis

AFM provides high-resolution, three-dimensional micrographs that reveal the surface topography at the nanoscale. This technique is employed to assess the texture, roughness, and porosity of concrete surfaces, which are critical factors in evaluating the mechanical performance of high-volume ceramic concrete composites. Fig. 14 showcase the AFM-derived surface morphologies of concrete specimens containing OPC, 60 % WTCP, and 4 % WBGNPs. In these images, darker areas indicate greater porosity, while lighter areas reflect higher peaks in surface topography.

The results indicate a notable decrease in porosity in the 28-day cured OPC specimens (Fig. 14 (a) right) compared to those cured for seven days (Fig. 14 (a) left), suggesting a denser and more compact microstructure due to increased formation of calcium-
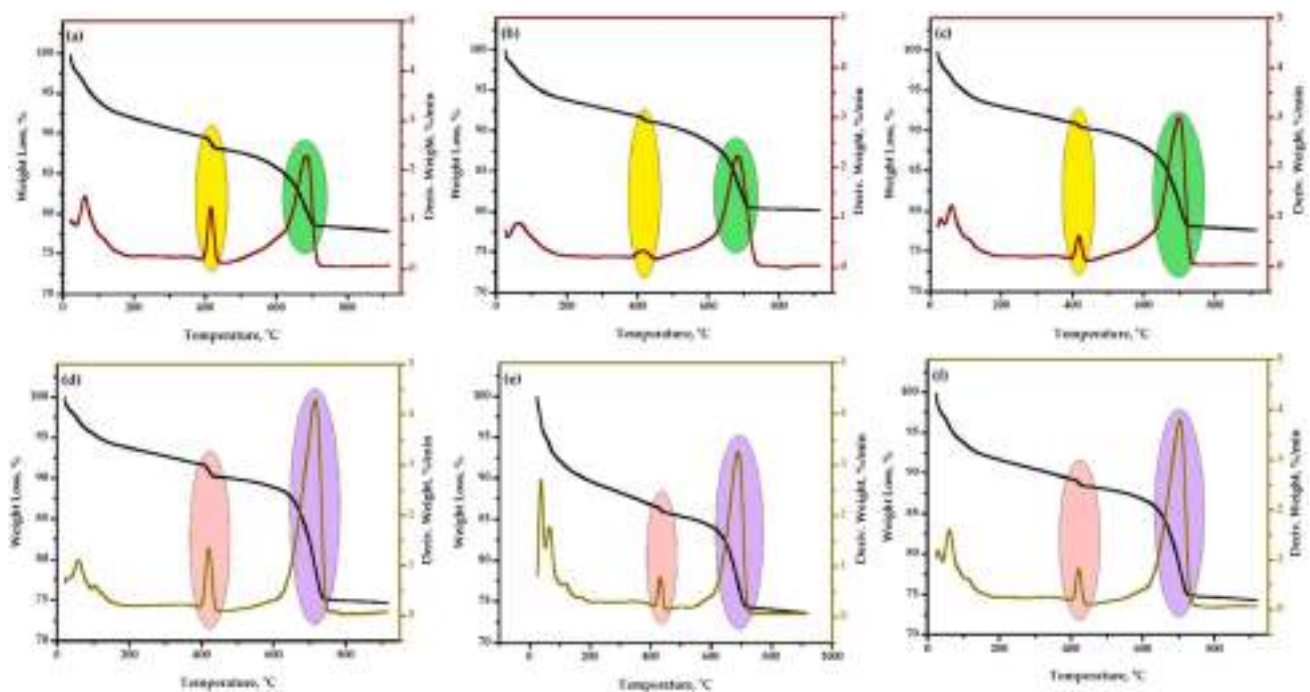

Fig. 13. TGA-DTG of (a) OPC specimens, (b) 60 % WTCPs, and (c) 4 % of WBGNPs at 7 days (d) OPC specimens, (e) 60 % WTCPs, and (f) 4 % of WBGNPs and 28 days(right) of curing age.

Table 4

TGA-DTG analysis results and dense gels and Portlandite formulation of OPC, 60 % WTCP, and 4 % WBGNPs at 7 and 28 days of curing age.

Proposed sample	Curing age, day	Dense gels, %	Portlandite, %
OPC (control sample)	7	12.67	9.86
	28	14.15	7.81
60WTCP	7	10.04	4.52
	28	12.64	5.75
4NPs	7	12.14	4.96
	28	13.91	6.08

aluminate-silicate-hydrate (C-A-S-H) gels. This reaction between SiO_2 and Al_2O_3 from pozzolanic materials with $Ca(OH)_2$ in OPC leads to improved mechanical properties. Conversely, the 60 % WTCP specimens (Fig. 14 (b)) exhibited a smoother surface, implying lower bond strength and corroborating the previously discussed compressive strength results.

Specimens containing 4 % WBGNPs (Fig. 14 (c)) showed significant improvements in surface density and roughness, indicating enhanced mechanical properties. A rougher surface generally suggests higher grain-boundary sliding, yet in this context, it indicates a more interlocked microstructure conducive to higher strength [78,79]. For instance, specimens with 4 % silica nanoparticles exhibited a roughness average (Ra) of 156.861 nm, indicative of a rougher, more textured surface compared to specimens without nanoparticles, which showed a Ra value of 0.236 nm. This textured surface translates to a better mechanical interlock at the paste-aggregate interface, enhancing the overall structural integrity of the concrete [80,81].

4.4. X-ray diffraction patterns analysis

The influence of silica nanoparticles on the microstructural performance of high-volume tile ceramic cement was investigated through XRD analysis at 7 and 28 days, with results showcased in Fig. 15. At the early stage of 7 days, the addition of 4 % WBGNPs significantly enhanced the hydration process, leading to increased dissolution of calcium, silica, and aluminum oxides and the subsequent formation of calcium hydroxide and calcium-alumino-silicate-hydrate (C-(A)-S-H) gels [82,83]. This enhancement in hydration and gel formation contributed to a substantial increase in the compressive strength of the concrete from 19.9 MPa to 29.2 MPa, as illustrated in Fig. 15(a).

The XRD analysis indicated a notable increase in the intensity of crystalline calcium hydroxide peaks at 18°, 29°, 37°, and 60° due to the presence of silica nanoparticles. Additionally, there was a noticeable reduction or replacement of quartz peaks by peaks indicative of calcium hydroxide, dicalcium silicate, and tricalcium silicate, suggesting a more active hydration process and denser gel formation facilitated by the nanoparticles.

At 28 days, similar enhancements were observed. The inclusion of silica nanoparticles continued to accelerate the hydration process, augment gel formation, and reduce porosity within the matrix. These microstructural improvements were evidenced by the increased compressive strength of the high-volume ceramic-cement specimens from 26.4 MPa to 36.9 MPa, as depicted in Fig. 15(b). This demonstrates the significant role of nanoparticles in optimizing the mechanical and microstructural properties of ceramic-based cement, confirming their potential for enhancing durability and strength in concrete applications [83–85].

5. Informational model to estimate the compressive strength

The application of Artificial Intelligence (AI) in the construction industry, particularly in concrete research, has seen a significant upsurge in recent years. This surge is driven by the need to optimize material properties, reduce experimental costs, and accurately predict the performance of concrete under various conditions. Recent studies have demonstrated the effectiveness of AI techniques in achieving these objectives, marking a pivotal shift in how concrete mixtures are designed and evaluated.

Convolutional Neural Networks (CNN) excel in predicting concrete compressive strength due to their spatial data processing capabilities [86]. DC Feng et al. highlight machine learning's role in forecasting concrete durability, showcasing the effectiveness of Random Forest and Gradient Boosting [87]. Rodriguez et al. explore Artificial Neural Networks (ANN) utility in modeling the strength of recycled aggregate concrete, emphasizing ANN's capability to navigate complex data relationships [88]. Furthermore, Li et al. validate the superiority of machine learning techniques over traditional regression analysis for concrete strength prediction, with ensemble methods like Random Forest providing significant accuracy improvements [89]. A Dinesh et al. review the impact of predictive analytics on concrete technology, illustrating how big data and AI models like Random Forest and Deep Learning can revolutionize concrete mix design and property prediction[90].

In summary, integrating AI into concrete research enhances the accuracy of predictive models and fosters innovation and sustainability in material design. As evidenced by the studies above, these advancements are instrumental in propelling the concrete industry toward more optimized and reliable material solutions. This section aims to harness the power of the Random Forest Regressor to predict the compressive strength of concrete mixtures accurately. It seeks to demonstrate the potential of AI in enhancing the quality and sustainability of concrete, contributing to the advancement of construction materials through innovative AI applications.
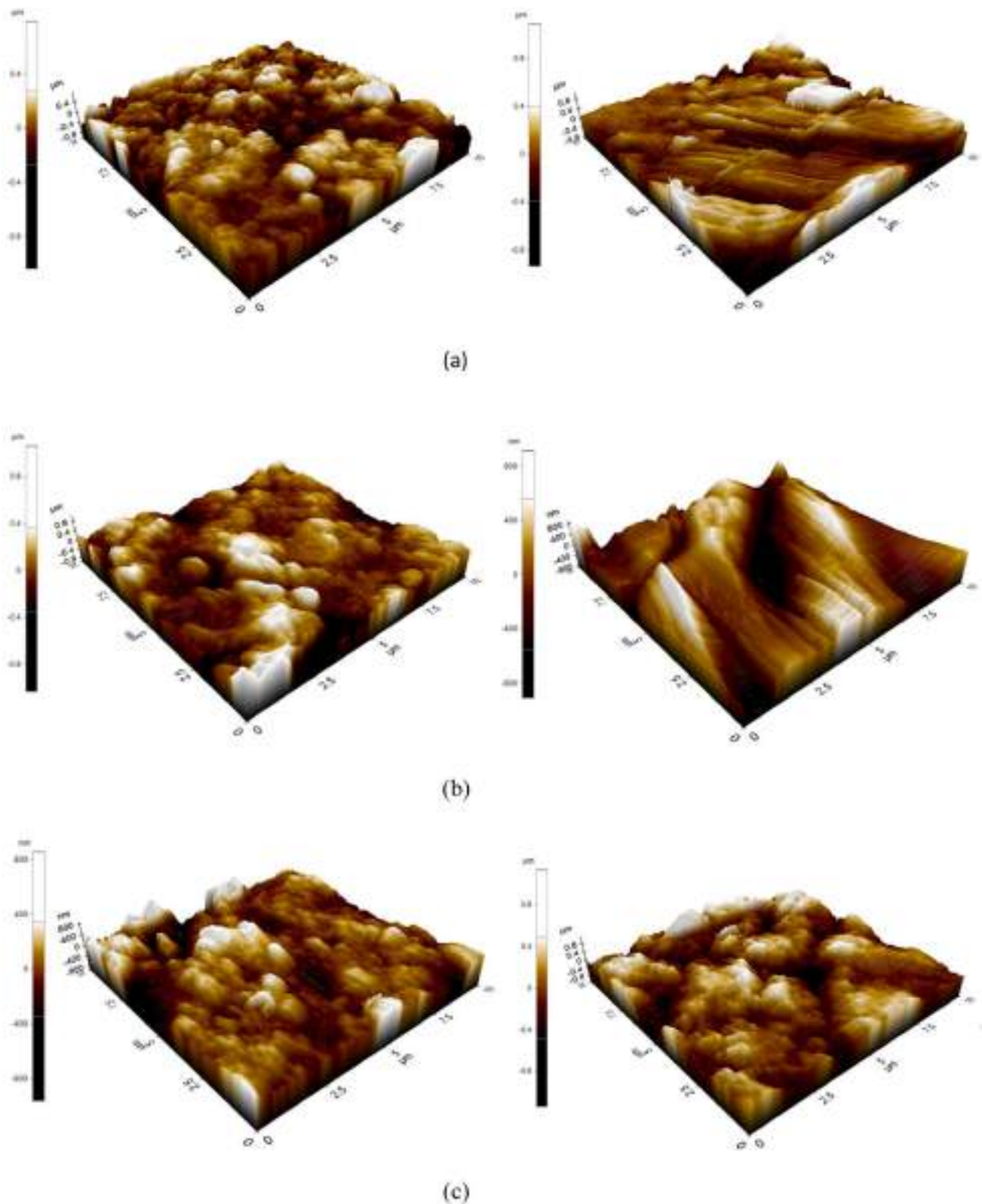
Fig. 14. AFM of (a)OPC specimens, (b) 60 % WTCPs, and (c) 4 % silica nanoparticle at 7 days (left) and 28 days (right) of curing age.

5.1. Dataset description

The dataset provided for this study comprises detailed mix designs of concrete samples, incorporating various materials and their respective quantities. The dataset encompasses a range of values for each parameter, ensuring a comprehensive analysis that accounts
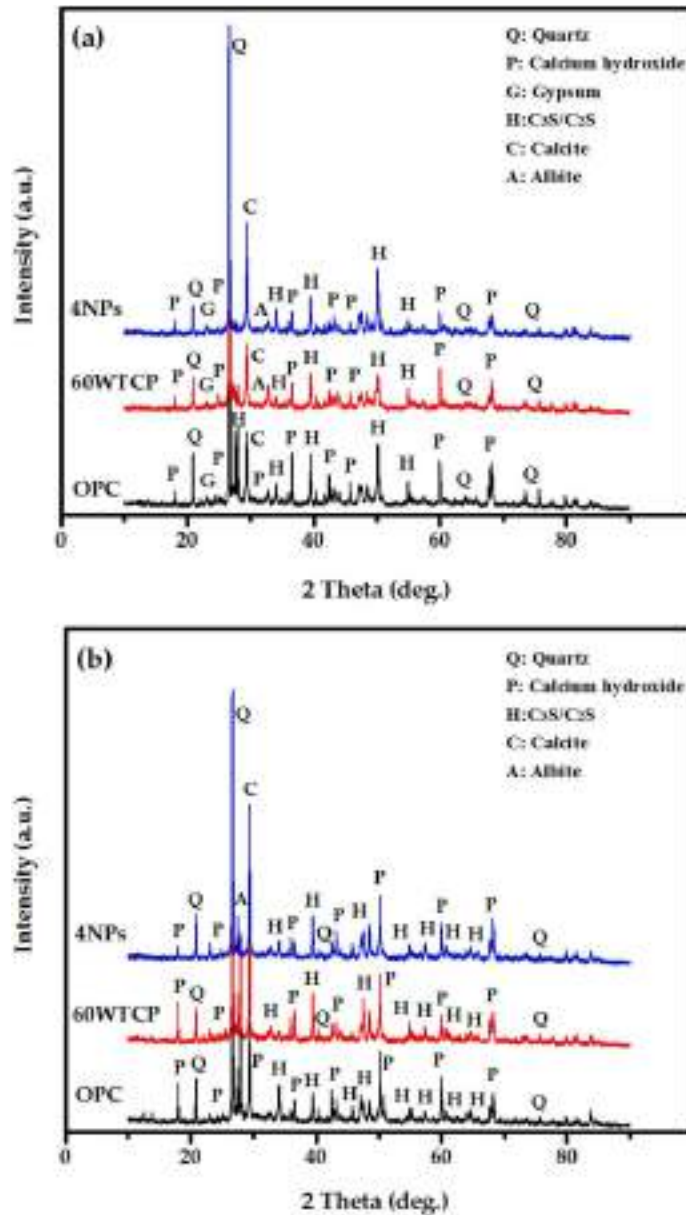
Fig. 15. XRD analysis of modified concrete with 60WTCP and 4 % WBGNPs at (a) 7 days, and (b) 28 days of curing ages.

for diverse mix proportions and their effects on compressive strength. Table 5 shows the dataset and summarizes each parameter's maximum, minimum, and average values, providing insights into the dataset's composition.

This rich dataset forms the foundation of our study, enabling the application of the Random Forest Regressor to predict the compressive strength of concrete samples accurately. By analyzing these varied mix designs, this research aims to uncover significant correlations between concrete ingredients and their compressive strength, thereby contributing valuable knowledge to the field of concrete technology.

The correlation matrix plot (Fig. 16) reveals insightful relationships between concrete mixture components and compressive strength. Key observations include the positive impact of cement content on strength, the beneficial use of glass powders as cement replacements, and the crucial role of the water-to-cement ratio and superplasticizers in influencing concrete's structural integrity.

5.2. Applied method

In this study, the Random Forest Regressor, an ensemble learning technique, was utilized to estimate the compressive strength of concrete mixtures. The model, leveraging its ensemble approach, constructs multiple decision trees, and the final prediction is obtained by averaging the predictions from all trees, which are mathematically represented $\bar{y} = \frac{1}{N} \sum_{i=1}^{N} T_{i(X)}$. This method allows for a nuanced capture of the complex, non-linear relationships within the data, a critical aspect given the diverse components influencing concrete's compressive strength.

Table 5
Summary Statistics of the Dataset Parameters.

Statistic	Mean	Max	Min
Cement	249.10	420.00	126.00
Ceramic powder	170.90	294.00	0.00
Nano-glass powder	4.34	42.00	0.00
Fine aggregates	70.34	816.00	0.00
Coarse aggregates	77.07	894.00	0.00
Fine ceramics	745.66	816.00	0.00
Coarse ceramics	816.93	894.00	0.00
Water to cement	0.51	0.55	0.42
Superplasticizer	0.83	2.00	0.00
Compressive strength	29.58	43.90	18.30
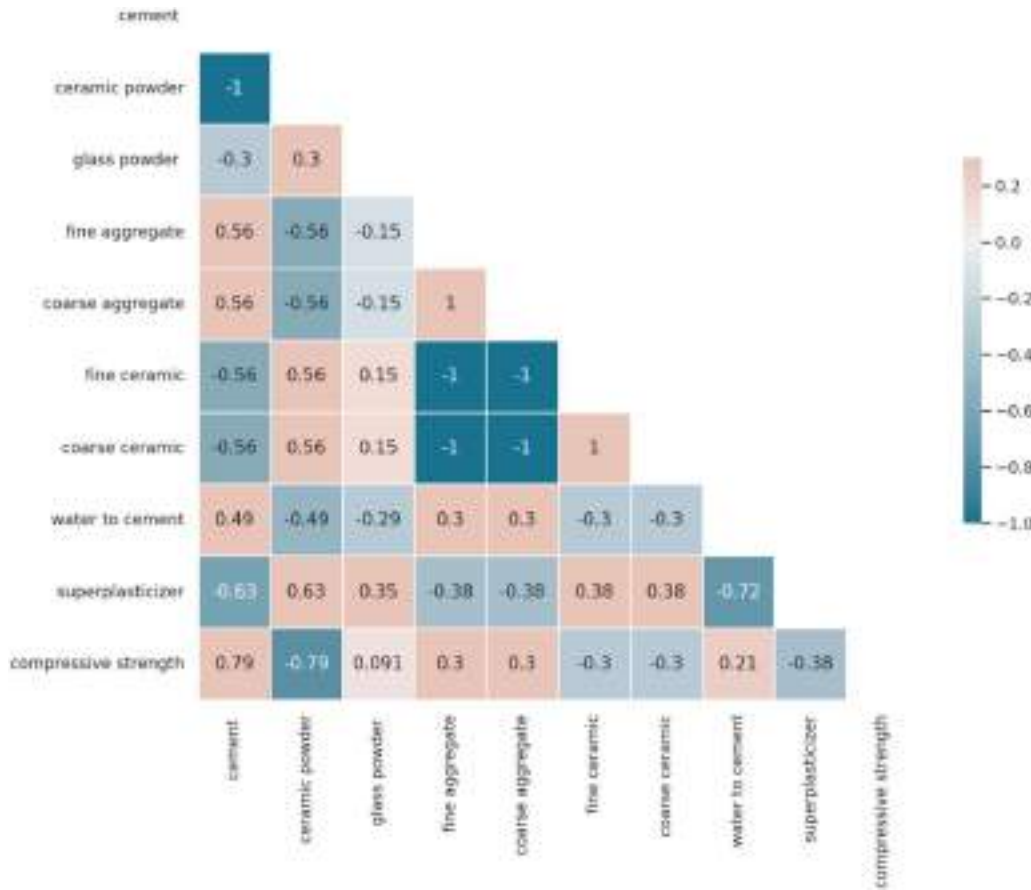
Fig. 16. Correlation matrix plot of the dataset.

The efficacy of the Random Forest model in predicting compressive strength was assessed using the coefficient of determination (R^2) and Mean Absolute Error (MAE), which gauges the model's accuracy and reliability. Fig. 17 shows a flowchart detailing each step, from data preprocessing to the final model evaluation, to facilitate understanding of the methodological process.

5.3. Results and discussion

The scatter plot in Fig. 18 illustrates the relationship between the experimental compressive strength and the values estimated by the Random Forest model. Each point on the plot corresponds to a concrete sample from the dataset, with the horizontal axis denoting the experimentally measured compressive strength and the vertical axis representing the strength estimated by the model. The proximity of the data points to the dashed line, which means a perfect match between the experimental and predicted values, indicates a high level of accuracy in the model's estimations. The coefficient of determination value of 0.92 further confirms the model's predictive strength, demonstrating that the Random Forest algorithm can reliably estimate the compressive strength based on the input parameters used in this study.

The sensitivity analysis plot generated using the Random Forest Regressor model, Fig. 19, reveals the relative importance of various
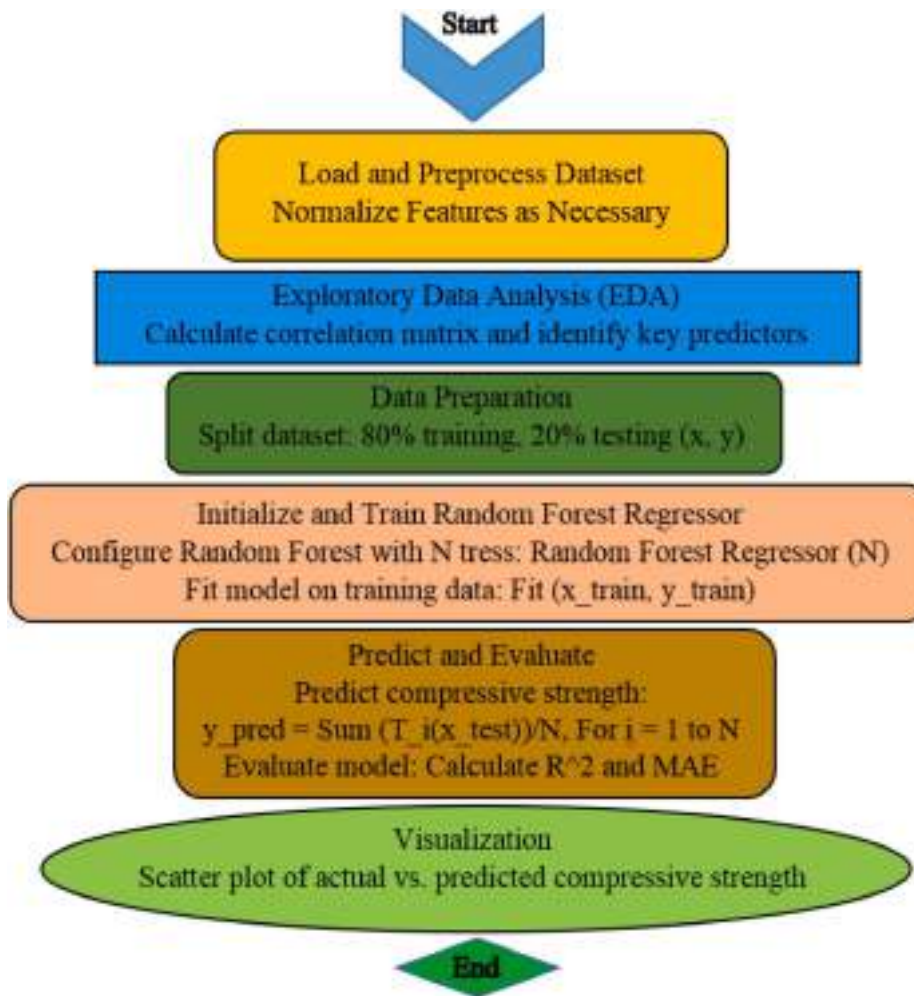
Fig. 17. Pseudo Flowchart of the Methodology for Estimating Compressive Strength Using the Random Forest Regressor.
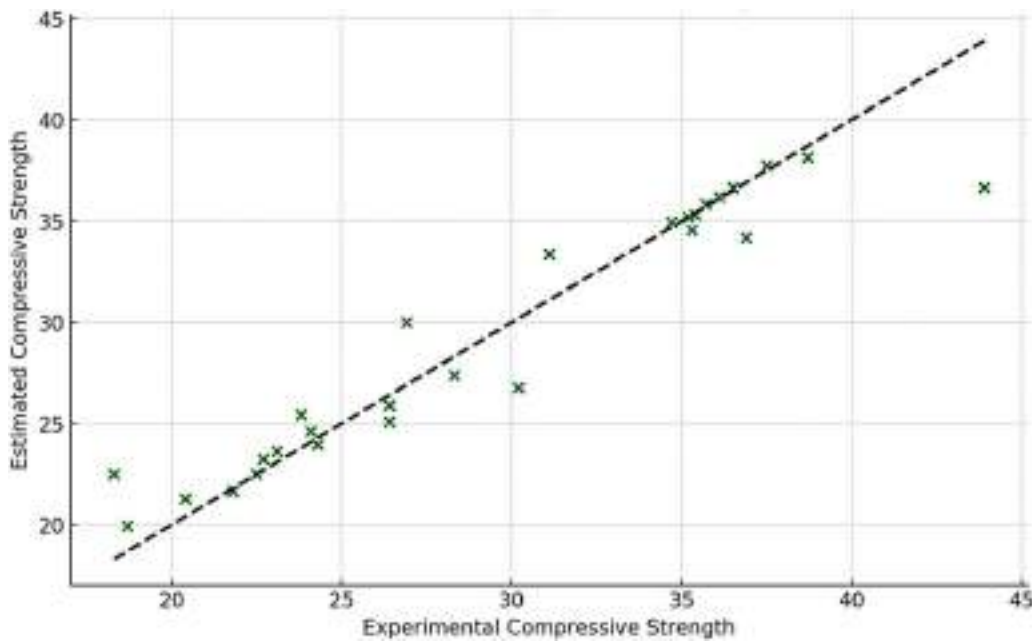

Fig. 18. Scatter plot comparing experimental and Random Forest estimated compressive strength.
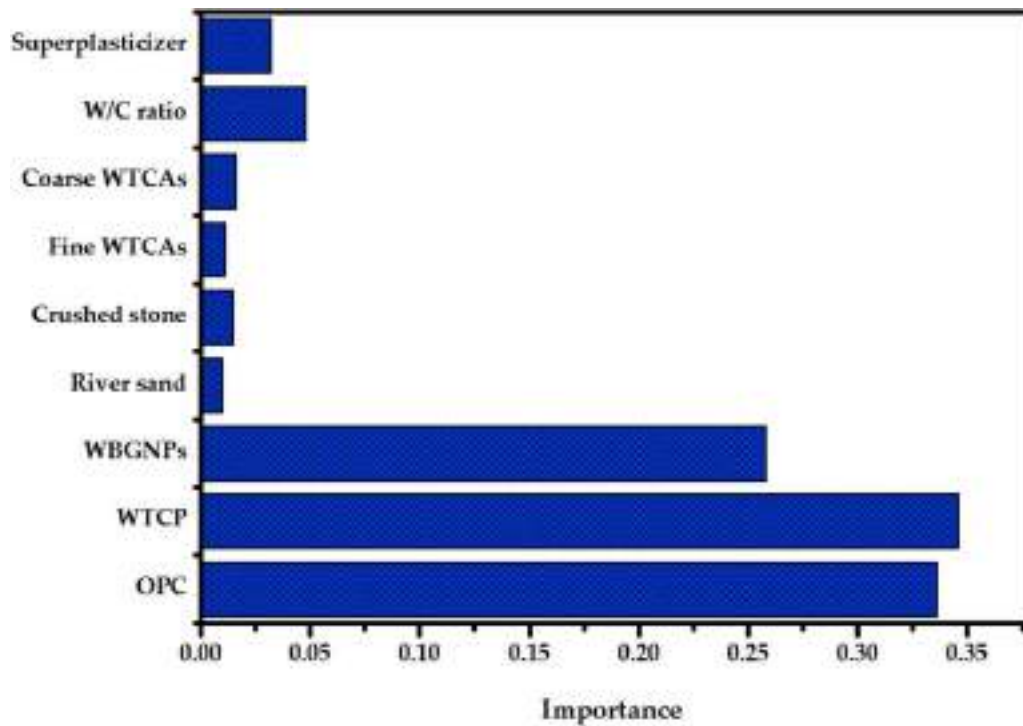
Fig. 19. Sensitivity analysis of concrete parameters using Random Forest.

parameters in predicting the compressive strength of concrete. Notably, certain features such as OPC, WTCP, WBGNPs content, and water-to-cement ratio exhibit a higher degree of influence on compressive strength, indicating their critical role in the mix design. The presence of ceramic powder and glass powder as partial replacements for cement also shows a considerable impact, suggesting their potential to enhance or maintain strength while contributing to sustainability. Conversely, other parameters like coarse aggregate and superplasticizer, while important, have a lesser impact on the predictive model.

6. Conclusions

This study has yielded several insightful conclusions regarding the use of WTCAs, WTCP and WBGNPs in concrete:

   i. Replacing natural aggregates with 100 % waste ceramic significantly boosts compressive strength at both early and late ages, demonstrating a sustainable approach that reduces natural resource use, landfill impacts, and CO_2 emissions.
   ii. The inclusion of waste tile ceramic powder (WTCP) at 10 %, 20 %, and 30 % as ordinary Portland cement (OPC) replacement markedly enhances compressive strength after 28 days. However, higher replacement levels above 30 % diminish strength, with 60 % WTCP achieving 22.5 MPa and 70 % reducing it further to 18.3 MPa at 28 days.
   iii. The optimal performance in compressive strength was observed in specimens with a water-cement ratio of 0.48 and 1.5 % superplasticizer, surpassing other mixtures at both early and late stages.
   iv. High-volume ceramic concrete incorporating varying levels of silica nanoparticles from waste bottle glass exemplifies a sustainable construction material, offering significant strength improvements.
   v. The strength of concrete is significantly influenced by the content of waste ceramic powder. While replacing 60 % of cement with WTCP generally reduces early and late strength by 47.2 % and 30.6 % respectively, the addition of 4 % silica nanoparticles optimizes and elevates strength by 39.7 % at 28 days compared to high-volume ceramic mixtures.
   vi. Enhancements were also observed in splitting tensile and flexural strengths, where the addition of 4 % silica nanoparticles considerably improved performance at 7 and 28 days.
   vii. Microstructural analyses using FESEM, EDX, TGA, DTG, and AFM reveal that silica nanoparticles significantly refine the gel formation, decrease pores and non-reactive particles, and enhance the bond strength within the paste, leading to improved mechanical properties.
   viii. Utilizing a Random Forest Regressor, this study successfully predicted concrete compressive strength with a high correlation coefficient of 0.92 between estimated and experimental values. This highlights the pivotal role of specific mix components in determining strength and underscores the potential of artificial intelligence in optimizing concrete formulations for enhanced performance and sustainability.

7. Recommendations for future research

Based on the obtained results of this experimental work, several recommendations for future research are highlighted as follows:

i. It's highly recommended to evaluate the high volume ceramic concrete' structural performance under different type of loads.
ii. The corrosion performance of the proposed concrete should be studied and widely evaluated.
iii. Effect of different type of nanomaterials on performance of high volume ceramic concrete high recommended to assess.
iv. The effect of various dosages and types of natural fibers on proposed concrete is highly recommended to develop concrete with high ductility performance for several applications in the construction industry.

CRediT authorship contribution statement

Adrina Rosseira A. Talip: Data curation, Software, Validation. **Iman Faridmehr:** Validation, Software, Formal analysis. **Zahraa Hussein Joudah:** Writing – original draft, Methodology, Conceptualization. **Nur Hafizah A. Khalid:** Visualization, Resources, Investigation. **Mohammad Hajmohammadian Baghban:** Writing – review & editing, Resources, Project administration, Funding acquisition. **Ghasan Fahim Huseien:** Writing – review & editing, Validation, Methodology.

Declaration of Competing Interest

The authors declare that there are no conflicts of interest regarding the publication of this paper. All authors have contributed significantly to this research and are in agreement with the content of the manuscript. The research was conducted without any commercial or financial relationships that could be construed as a potential conflict of interest. The study was performed solely for the advancement of scientific knowledge and the promotion of sustainable construction practices.

Data availability

Data will be made available on request.

Acknowledgment

Abbreviations

CO_2: Carbon dioxide
C-S-H: Calcium silicate hydrate
FESEM: Field emission scanning electron microscopy
OPC: Ordinary Portland cement
SCMs: Supplementary cementitious materials
SP: Superplasticizer
W/C: Water to cement ratio
WBGNPs: Wastes bottle glass nanoparticles
WTCA: Waste tile ceramic aggregates
WTCP: Waste tile ceramic powder
XRD: X-ray diffraction
XRF: X-ray fluorescence

References

[1] S. Deetman, et al., Modelling global material stocks and flows for residential and service sector buildings towards 2050, J. Clean. Prod. 245 (2020) 118658.
[2] D.C. Reis, et al., *Potential CO_2 reduction and uptake due to industrialization and efficient cement use in Brazil by 2050.* J. Ind. Ecol. 25 (2) (2021) 344–358.
[3] K.A. Knight, P.R. Cunningham, S.A. Miller, Optimizing supplementary cementitious material replacement to minimize the environmental impacts of concrete, Cem. Concr. Compos. 139 (2023) 105049.
[4] K.M. Rahla, R. Mateus, L. Bragança, Comparative sustainability assessment of binary blended concretes using Supplementary Cementitious Materials (SCMs) and Ordinary Portland Cement (OPC), J. Clean. Prod. 220 (2019) 445–459.
[5] S. Gupta, S. Chaudhary, State of the art review on supplementary cementitious materials in India–II: Characteristics of SCMs, effect on concrete and environmental impact. J. Clean. Prod. 357 (2022) 131945.
[6] M.S. Fattouh, et al., Improvement in the flexural behaviour of road pavement slab concrete containing steel fibre and silica fume, Case Stud. Constr. Mater. 18 (2023) e01720.
[7] I.Y. Hakeem, et al., Properties of sustainable high-strength concrete containing large quantities of industrial wastes, nanosilica and recycled aggregates, J. Mater. Res. Technol. 24 (2023) 7444–7461.
[8] M.H. Abd-Elrahman, et al., Effect of utilizing peanut husk ash on the properties of ultra-high strength concrete, Constr. Build. Mater. 384 (2023) 131398.
[9] M.H. Abd-Elrahman, et al., Effect of utilising ferrosilicon and recycled steel fibres on ultra-high-strength concrete containing recycled granite, Case Stud. Constr. Mater. 18 (2023) e01903.

[10] I.Y. Hakeem, et al., Using a combination of industrial and agricultural wastes to manufacture sustainable ultra-high-performance concrete, Case Stud. Constr. Mater. 19 (2023) e02323.
[11] K.K. Sahoo, et al., Influence of ground-granulated blast-furnace slag on the structural performance of self-compacting concrete, Pract. Period. Struct. Des. Constr. 27 (3) (2022) 04022019.
[12] D. Ndahirwa, et al., The role of supplementary cementitious materials in hydration, durability and shrinkage of cement-based materials, their environmental and economic benefits: A review, Clean. Mater. 5 (2022) 100123.
[13] V.P. Kumar, S. Dey, Study on strength and durability characteristics of nano-silica based blended concrete, Hybrid. Adv. 2 (2023) 100011.
[14] B. Pacewska, I. Wilińska, Usage of supplementary cementitious materials: Advantages and limitations: Part I. C–S–H, C–A–S–H and other products formed in different binding mixtures, J. Therm. Anal. Calorim. 142 (1) (2020) 371–393.
[15] R. Snellings, P. Suraneni, J. Skibsted, Future and emerging supplementary cementitious materials, Cem. Concr. Res. 171 (2023) 107199.
[16] V.P. Kumar, D.R. Prasad, Influence of supplementary cementitious materials on strength and durability characteristics of concrete, Adv. Concr. Constr. 7 (2)) (2019) 75.
[17] W.E. Elemam, I.S. Agwa, A.M. Tahwia, Reusing ceramic waste as a fine aggregate and supplemental cementitious material in the manufacture of sustainable concrete, Buildings 13 (11) (2023) 2726.
[18] M. Amin, et al., Effect of industrial wastes on the properties of sustainable ultra-high-performance concrete: Ganite, ceramic, and glass, Constr. Build. Mater. 428 (2024) 136292.
[19] A. Alsaif, Utilization of ceramic waste as partially cement substitute–A review. Constr. Build. Mater. 300 (2021) 124009.
[20] D.M. Kannan, et al., High performance concrete incorporating ceramic waste powder as large partial replacement of Portland cement, Constr. Build. Mater. 144 (2017) 35–41.
[21] X. Chen, et al., Sustainable reuse of ceramic waste powder as a supplementary cementitious material in recycled aggregate concrete: Mechanical properties, durability and microstructure assessment, J. Build. Eng. 52 (2022) 104418.
[22] L. Li, et al., A study of some relevant properties of concrete incorporating waste ceramic powder as a cement replacement agent, J. Build. Eng. 87 (2024) 109106.
[23] J. Silvestre, N. Silvestre, J. De Brito, Review on concrete nanotechnology, Eur. J. Environ. Civ. Eng. 20 (4) (2016) 455–485.
[24] Z. Luo, et al., Current progress on nanotechnology application in recycled aggregate concrete, J. Sustain. Cem. -Based Mater. 8 (2) (2019) 79–96.
[25] M.J. Hanus, A.T. Harris, Nanotechnology innovations for the construction industry, Prog. Mater. Sci. 58 (7) (2013) 1056–1102.
[26] H.K. Hamzah, et al., Effect of waste glass bottles-derived nanopowder as slag replacement on mortars with alkali activation: Durability characteristics, Case Stud. Constr. Mater. 15 (2021) e00775.
[27] G.F. Huseien, et al., Structure, morphology and compressive strength of Alkali-activated mortars containing waste bottle glass nanoparticles, Constr. Build. Mater. 342 (2022) 128005.
[28] M. Samadi, et al., Enhanced performance of nano-palm oil ash-based green mortar against sulphate environment, J. Build. Eng. 32 (2020) 101640.
[29] A.A. Ramezanianpour, M. Mortezaei, S. Mirvalad, Synergic effect of nano-silica and natural pozzolans on transport and mechanical properties of blended cement mortars, J. Build. Eng. 44 (2021) 102667.
[30] ASTM, C., ASTM C150: Standard specification for Portland cement. American Society for Testing and Materials, West Conshohocken, PA, 2001.
[31] I. Kang, S. Shin, J. Kim, Optimal Limestone Content on Hydration Properties of Ordinary Portland Cement with 5% Ground Granulated Blast-Furnace Slag, Materials 17 (13) (2024) 3255.
[32] C. Astm, Standard specification for coal fly ash and raw or calcined natural pozzolan for use as a mineral admixture in concrete, Annu. Book ASTM Stand. *618* (2005) 4.
[33] C. Astm, Standard test method for sieve analysis of fine and coarse aggregates, ASTM C136-06 (2006).
[34] A. ASTM, Standard test method for relative density (specific gravity) and absorption of coarse aggregate, ASTM West Conshohocken, PA (2015).
[35] Berney, E.S. and D.M. Smith, Mechanical and physical properties of ASTM C33 Sand. 2008.
[36] C128–15, A., Standard test method for relative density (specific gravity) and absorption of fine aggregate. ASTM Int., 2015. 1: p. 2–7..
[37] ASTM, M., C579 Standard Test Methods for Compressive Strength of Chemical-Resistant Mortars. Grouts, Monolithic Surfacings, and Polymer Concretes, 2001..
[38] Standard, A., C143 (2015) Standard test method for slump of hydraulic-cement concrete. ASTM International, West Conshohocken..
[39] ASTM, A., C109/109M. Standard Test Method for compressive Strength of Hydraulic Cement Mortars (Using 2-In. or [50-mm] Cube Specimens), 2020..
[40] Standard, A., C496/C496M-11. Standard Test Method for Splitting Tensile Strength of Cylindrical Concrete Specimens, 2004..
[41] A. Peled, J. Castro, W. Weiss, Atomic force and lateral force microscopy (AFM and LFM) examinations of cement and cement hydration products, Cem. Concr. Compos. 36 (2013) 48–55.
[42] G.F. Huseien, et al., Alkali-activated mortars blended with glass bottle waste nano powder: Environmental benefit and sustainability, J. Clean. Prod. 243 (2020) 118636.
[43] G.F. Huseien, A review on concrete composites modified with nanoparticles, J. Compos. Sci. 7 (2) (2023) 67.
[44] A.O. Tanash, et al., A review on the utilization of ceramic tile waste as cement and aggregates replacement in cement based composite and a bibliometric assessment, Clean. Eng. Technol. (2023) 100699.
[45] F. Xu, et al., Effects of recycled ceramic aggregates on internal curing of high performance concrete, Constr. Build. Mater. 322 (2022) 126484.
[46] M. Samadi, et al., Waste ceramic as low cost and eco-friendly materials in the production of sustainable mortars, J. Clean. Prod. 266 (2020) 121825.
[47] E. Lasseuguette, et al., Chemical, microstructural and mechanical properties of ceramic waste blended cementitious systems, J. Clean. Prod. 211 (2019) 1228–1238.
[48] G. Matias, P. Faria, I. Torres, Lime mortars with heat treated clays and ceramic waste: A review, Constr. Build. Mater. 73 (2014) 125–136.
[49] G.F. Huseien, et al., Impact resistance enhancement of sustainable geopolymer composites using high volume tile ceramic wastes, J. Compos. Sci. 7 (2) (2023) 73.
[50] R.P. Memon, et al., Microstructure and Strength Properties of Sustainable Concrete Using Effective Microorganisms as a Self-Curing Agent, Sustainability 14 (16) (2022) 10443.
[51] R.P. Memon, et al., A review: Mechanism, materials and properties of self-curing concrete, ARPN J. Eng. Appl. Sci. 13 (2018) 9304–9397.
[52] G.F. Huseien, et al., Effective microorganism solution-imbued sustainable self-curing concrete: Evaluation of sorptivity, drying shrinkage and expansion, Case Stud. Constr. Mater. 20 (2024) e03255.
[53] N. Hamzah, et al., A review on the use of self-curing agents and its mechanism in high-performance cementitious materials, Buildings 12 (2) (2022) 152.
[54] A.M. Onaizi, et al., Effect of the addition of nano glass powder on the compressive strength of high volume fly ash modified concrete, Mater. Today.: Proc. 48 (2022) 1789–1795.
[55] M. Samadi, et al., Influence of glass silica waste nano powder on the mechanical and microstructure properties of alkali-activated mortars, Nanomaterials 10 (2) (2020) 324.
[56] D.-Y. Yoo, T. Oh, N. Banthia, Nanomaterials in ultra-high-performance concrete (UHPC)–A review, Cem. Concr. Compos. 134 (2022) 104730.
[57] G.F. Huseien, K.W. Shah, A.R.M. Sam, Sustainability of nanomaterials based self-healing concrete: An all-inclusive insight, J. Build. Eng. 23 (2019) 155–171.
[58] Q. Shao, et al., Enhancement of nano-alumina on long-term strength of Portland cement and the relation to its influences on compositional and microstructural aspects, Cem. Concr. Compos. 98 (2019) 39–48.
[59] W. Li, et al., Effects of nanoalumina and graphene oxide on early-age hydration and mechanical properties of cement paste, J. Mater. Civ. Eng. 29 (9) (2017) 04017087.
[60] K. De Weerdt, et al., Hydration mechanisms of ternary Portland cements containing limestone powder and fly ash, Cem. Concr. Res. 41 (3) (2011) 279–291.
[61] Y. Feng, et al., Effects of recycled sand and nanomaterials on ultra-high performance concrete: Workability, compressive strength and microstructure, Constr. Build. Mater. 378 (2023) 131180.

[62] J.A. Abdalla, et al., Influence of nanomaterials on the workability and compressive strength of cement-based concrete, Mater. Today.: Proc. 65 (2022) 2073–2076.

[63] A.M. Onaizi, et al., Effect of nanomaterials inclusion on sustainability of cement-based concretes: A comprehensive review, Constr. Build. Mater. 306 (2021) 124850.

[64] V. López-Carrasquillo, S. Hwang, Comparative assessment of pervious concrete mixtures containing fly ash and nanomaterials for compressive strength, physical durability, permeability, water quality performance and production cost, Constr. Build. Mater. 139 (2017) 148–158.

[65] Z. Luo, et al., Effects of different nanomaterials on the early performance of ultra-high performance concrete (UHPC): C–S–H seeds and nano-silica, Cem. Concr. Compos. 142 (2023) 105211.

[66] G.F. Huseien, N.H.A. Khalid, J. Mirza, Nanotechnology for smart concrete, CRC Press, 2022.

[67] S. Nazar, et al., Formulation of estimation models for the compressive strength of concrete mixed with nanosilica and carbon nanotubes, Dev. Built Environ. 13 (2023) 100113.

[68] N. Bheel, et al., A comprehensive study on the impact of nano-silica and ground granulated blast furnace slag on high strength concrete characteristics: RSM modeling and optimization. *Structures*, Elsevier, 2024.

[69] M. Ünal, et al., Nanomaterial and fiber-reinforced sustainable geopolymers: A systematic critical review, Constr. Build. Mater. 404 (2023) 133325.

[70] H.U. Ahmed, et al., Compressive strength of geopolymer concrete modified with nano-silica: Experimental and modeling investigations, Case Stud. Constr. Mater. 16 (2022) e01036.

[71] M. Ebrahimi, et al., Effect of ceramic waste powder as a binder replacement on the properties of cement-and lime-based mortars, Constr. Build. Mater. 379 (2023) 131146.

[72] C. Fan, et al., Study on mechanical and bonding properties of nano-SiO2 reinforced recycled concrete: macro test and micro analysis, J. Build. Eng. (2024) 109877.

[73] J.A. Abdalla, et al., Influence of synthesized nanomaterials in the strength and durability of cementitious composites, Case Stud. Constr. Mater. 18 (2023) e02197.

[74] H.-B. Tran, V.T.-A. Phan, Potential usage of fly ash and nano silica in high-strength concrete: Laboratory experiment and application in rigid pavement, Case Stud. Constr. Mater. 20 (2024) e02856.

[75] M.V. Rao, R. Sivagamasundari, T.V. Nagaraju, *Achieving strength and sustainability in ternary blended Concrete: leveraging industrial and agricultural By-Products with controlled Nano-SiO₂ content.* Clean. Mater. 9 (2023) 100198.

[76] N.N.A. Rasid, et al., Ground palm oil fuel ash and calcined eggshell powder as SiO2–CaO based accelerator in green concrete. J. Build. Eng. 65 (2023) 105617.

[77] A.N. Saleh, et al., Comparative study of the effect of silica nanoparticles and polystyrene on the properties of concrete, Results Mater. 18 (2023) 100405.

[78] M. Miller, et al., Surface roughness criteria for cement paste nanoindentation, Cem. Concr. Res. 38 (4) (2008) 467–476.

[79] Z. Wang, et al., Strength, toughness and interface modification of graphene oxide grafted carbon fiber modified concrete, Constr. Build. Mater. 428 (2024) 136336.

[80] A.M. Mhaya, et al., Effect of metakaolin content and shape design on strength performance of lightweight rubberized geopolymer mortars incorporated slag-waste glass powders, Constr. Build. Mater. 432 (2024) 136500.

[81] H.A. Algaifi, et al., Optimizing durability and performance in high-volume fly ash-based alkali-activated mortar with palm oil fuel ash and slag: A response surface methodology approach, Dev. Built Environ. 18 (2024) 100427.

[82] R.A. El-Sadany, H.E.-D.M. Sallam, S.H. Al-Tersawy, Effect of hybrid nanoparticles additions to normal weight concrete on its microstructures and mechanical properties before and after exposure to gamma-rays, Constr. Build. Mater. 376 (2023) 131037.

[83] M.H. Khan, et al., Evaluation of mechanical strength, gamma-ray shielding characteristics, and ITZ microstructural properties of heavyweight concrete using nano-silica (SiO2) and barite aggregates, Constr. Build. Mater. 419 (2024) 135483.

[84] D. Chekravarty, et al., Effect of using nano silica on mechanical properties of normal strength concrete, Mater. Today.: Proc. 51 (2022) 2573–2578.

[85] D. Wang, et al., Effects of nanomaterials on hardening of cement–silica fume–fly ash-based ultra-high-strength concrete, Adv. Cem. Res. 28 (9) (2016) 555–566.

[86] Z. Zeng, et al., Accurate prediction of concrete compressive strength based on explainable features using deep learning, Constr. Build. Mater. 329 (2022) 127082.

[87] D.-C. Feng, et al., Machine learning-based compressive strength prediction for concrete: An adaptive boosting approach, Constr. Build. Mater. 230 (2020) 117000.

[88] V. Rodriguez-Galiano, et al., Machine learning predictive models for mineral prospectivity: An evaluation of neural networks, random forest, regression trees and support vector machines, Ore Geol. Rev. 71 (2015) 804–818.

[89] D. Li, et al., Machine learning-based method for predicting compressive strength of concrete, Processes 11 (2) (2023) 390.

[90] A. Dinesh, B.R. Prasad, Predictive models in machine learning for strength and life cycle assessment of concrete structures, Autom. Constr. 162 (2024) 105412.